

The roles of Green Fluorescent Proteins and photo-acclimation on the physiological and behavioural responses of *Anemonia viridis*



Submitted by Matthew James Kyle-Henney, to the University of Exeter as a thesis for the degree of Master of Science by Research in Biological Sciences, June 2021.

This thesis is available for Library use on the understanding that it is copyright material and that no quotation from the thesis may be published without proper acknowledgement.

I certify that all material in this thesis which is not my own work has been identified and that any material that has previously been submitted and approved for the award of a degree by this or any other University has been acknowledged.

Signature:
1

Abstract

Studying the fundamental relationships between marine organisms is vital in determining the biological implications of changing environments. In many cases, these environments are underpinned by photosynthetic primary production, and directly affected by variation in abiotic stressors such as light condition and temperature. Photosymbiotic relationships between unicellular plants and multicellular animals are well studied, but their complexity and interspecies variation has resulted in many unanswered questions within physiology and behaviour. Respirometry is a well-known method in laboratory studies for quantifying physiological impacts of these stressors, however, commercially available respirometry equipment has significant limitations. Chapter 1 therefore describes a novel open source (OS) photo-respirometer to reduce these limitations, whilst maintaining comparable precision and accuracy to explore complex ecological relationships. A temperate example of the algae-cnidarian symbiosis was used to showcase the data collection ability of our photo-respirometer. Results suggest that the photosynthetic efficiency of *A. viridis* – *Symbiodinium* symbioses may be influenced by light intensity, acclimation condition and the presence or absence of green fluorescent proteins (GFPs). This first study concludes that the photo-respirometer is a viable alternative to commercial systems and would be advantageous as a single base apparatus for multiple metabolic studies within marine contexts. Chapter 2 then explores the behavioural implications of GFP expression and acclimation condition on phototactic responses of *A. viridis* to light intensity gradients. Acclimation to low light intensity elicited the greatest phototactic responses, but only when water flow direction and the light intensity gradient were opposed. Phototactic responses did not differ between morphs directly, suggesting that GFP expression may have alternative functions or be a vestigial trait in this species. Phototaxis was more heavily dependent on water flow direction, suggesting that either water movement or oxygen concentration is a limiting factor for phototaxis in temperate cnidarian-algal symbioses, and should be the focus of future studies.

List of Contents

1. Abstract	2
2. List of Tables and Figures	5
3. List of Accompanying Material	8
4. Authors Declaration	9
5. Acknowledgements	10
6. Definitions and Abbreviations	12
7. General Introduction	13
8. Chapter 1 - Open Source Respirometry: A Low-Cost, Versatile Apparatus for Collecting Metabolic Data on Small Marine Organisms	18
- Abstract	19
- Introduction	20
- Materials and Methods	21
- The Subject Organisms – photosymbiotic cnidaria	21
- Design Overview	22
- System Components	22
- Housing and Circulation	22
- Light Delivery	23
- Control System and User Interface	23
- System Testing	25
- GFP Example Investigation	25
- Results	26
- Discussion/Conclusion	26
- Figures	29
9. Chapter 2 - Phototaxis Behaviour in <i>Anemonia viridis</i> : Is Movement Influenced by GFP Expression and Acclimation Condition?	34
- Abstract	35
- Introduction	36
- Methods	38
- Animal collection and husbandry	38
- Phototaxis experiments	39
- Statistical analysis	40

- Results 41
 - Do individuals of *A. viridis* display positive phototaxis? 42
 - The effect of morph and acclimation condition on final positions after 6 days 42
 - How are phototactic responses influenced by acclimation condition? 42
- Discussion/Conclusion 43
- Figures and Tables 47
- 10. General Discussion/Conclusion 50**
- 11. Appendices 54**
- 12. Bibliography 58**

List of Tables and Figures

Chapter 1:

Figure 1: The basic layout of the respirometry system. The circulation pump provides constant water flow (black arrows) between the subject and measurement chambers during measurement phases. The flush pump controls water flow (grey arrows) between all chambers to replenish oxygen concentrations during rest/replenish phases. The oxygen sensor in the measurement chamber feeds information to the external datalogging system.

Figure 2: The LED housing that shrouds the subject chamber and converts the respirometer into a photo-respirometer. LEDs with sunlight-mimicking emission spectra project PAR at the subject from all sides and are cooled by metal heatsinks and electronic fans located in the 3 rectangular sections.

Figure 3: The full photo-respirometer system, including (from left to right): temperature regulating bath containing the reservoir; peristaltic water pumps (yellow box); small measurement chamber containing the oxygen sensor; subject chamber, with blue paper towel to eliminate any external light sources and lighting rig; and the oxygen sensor unit and RPi computer.

Figure 4: Raw data produced by our photo-respirometer, showing the change in oxygen concentration ($\mu\text{mol/L}$) over time (minutes) for two individual anemones and a control with no individual, and the associated PI curves. Specifically, A. shows the photosynthetic responses of a brown morph exposed to a full experimental period with 6 measurement phases, and B. shows the same individual exposed to a shorter measurement period. C. shows the responses of a green morph exposed to a full period, and D. shows the same green morph exposed to a shorter period. E. shows the change in oxygen concentration within the system with no individual in the subject chamber as a control for background flux. Light intensity was increased periodically and sustained for 10 minutes at a time, depicted by the black measurement phases, and oxygen concentration fluctuated during the grey recirculation phase as fresh water flushed the subject and measurement chambers (A. – E.).

Linear models were used to determine photosynthetic rates during the measurement phases for both individuals and the control, and plotted against the

corresponding light intensity ($\mu\text{mol photons/m}^2/\text{S}$) at each phase (F.). Black lines with triangular points represent the brown morph (in A. and B.), green lines with circular points represent the green morph (in C. and D.), and the grey line with square points represents the control 'blank' response (in E.). The gradient of the PI curves can be used to calculate photosynthetic efficiency.

Figure 5: The relationship between photosynthetic rate ($\mu\text{mol/L/min}$) and light intensity ($\mu\text{mol photons/m}^2/\text{S}$) for Brown (black) and Green (green) morphs that were acclimated to 4 conditions: high light and high food (HLHF), high light and low food (HLLF), low light and high food (LLHF), and low light and low food (LLLFB). Individual responses are represented by points and model fits represented by dashed lines. Mean responses for brown (black) and green (green) morphs under each condition are represented by thicker solid lines.

Figure 6: The parameter estimates of the Eilers PI curve model fitted to each group (including acclimation to high or low light, high or low food availability, and morph) within the example investigation data. The parameter 'Pmax' represents the photosynthetic maxima, 'lopt' represents the optimal light intensity, 'a' represents the predicted initial slope of the PI curve, and 'c' represents the y intercept. It is important to note that values in lopt are extrapolated, and some data was excluded from the plot as they lay outside an estimate value of 1000 (particularly in LLLFB). This can be rectified by increasing the value of light intensity during the measurement phases to cause photoinhibition, which would reduce the rate of photosynthesis from the optimal value and prevent excessive extrapolation by the non-linear model.

Chapter 2:

Figure 1: Distance moved towards the LED light source after 6 days for all groups when water flow is in the direction of positive movement (white bars) or in the direction of negative movement (grey bars). Groups relate to the acclimation condition (high light or low light) and morph (green or brown). The R in groups with grey shading refers to the direction of water flow being reversed. The number of individuals in each group ranges from 8 to 11 as a result of death or splitting (asexual reproduction) mid experiment. Black points outside the interquartile ranges are individual outliers, however at time of measurement the individuals

were attached to the surface so movement was achieved either by pedal disk motion or movement by the water current following detachment.

Figure 2: The displacement of green morphs (green) and brown morphs (black) from the starting point towards the light source over the 6-day period. Points show the raw positions of individuals that follow a non-linear pattern, with a regression line representing the mixed effect model used to observe differences between groups. a.) The responses of HL (left) and LL (right) acclimated individuals when positive phototaxis and water flow were concurrent. b.) The same individual responses when positive phototaxis and water flow were opposing. HL acclimated green individuals exhibit greater phototaxis responses than HL acclimated brown individuals regardless of water flow direction. Brown morphs exhibit greater phototaxis responses when acclimated to LL than HL, and their LL responses match that of LL green morphs. Reversing the direction of water flow increases the phototactic response of both green and brown morphs that have been LL acclimated.

Table 1: The lmer output for the opposing water flow trial. Estimate values indicate the fixed effect size and direction, supported by an F test for significance.

Table 2: The lmer output for the concurrent water flow trial. Estimate values indicate the fixed effect size and direction, supported by an F test for significance.

List of Accompanying Material

Chapter 1:

Figure A1: Technical drawing of the lighting rig housing with dimensions in mm. The depth and inner diameter of the housing is dependent on the size of the subject chamber being used and tolerances should be small enough to prevent light from entering the chamber when LEDs are off (~1mm).

RPi wiring diagram (weblink)

PicoBuck driver technical sheet (weblink)

Table A1: Pin layout of the RPi with corresponding function and which input and output pins have been utilised by our system. The high number of pins shows how versatile the RPi is as an OS system, and the potential for complex systems to be created.

Chapter 2:

Figure A2: Experimental setup for phototaxis trials. 5 individuals (in this case green morphs at day 1) were positioned 750 mm from the midpoint of the LED light source (0 mm). Light intensity increased as distance towards the LEDs decreased. Blue circles represent the water input (left) and output (right) pipes that created a steady continuous water flow from left to right. The vertical grid was used to calculate the position of individuals per day.

Figure A3: The individual phototaxis responses over a period of 6 days, overlaid with fitted values (i.e., model predictions). A nonlinear logistic model was used to explain the pattern of movement, fitted using lmer in Rstudio. This figure shows the potential for individual preference to be an important factor when investigating phototaxis responses. Investigating these preferences were beyond the scope of this investigation but are a sound foundation for future studies.

Author's Declaration

All data collection was conducted by myself and Dr Chris Lowe in accordance with the University of Exeter's regulations and ethical guidelines, supervised by Dr Chris Lowe and Professor Alastair Wilson.

Chapter 1's data was collected by Dr Chris Lowe due to COVID 19 restrictions and other laboratory issues that prevented me from entering the laboratory. Chapter 2's experimental design and data collection was conducted by me in all aspects. Data analysis was conducted by me with supervisory input from Dr Chris Lowe and guidance from Professor Alastair Wilson. The collation of research, manuscript/thesis writing, and formatting was conducted by myself, with significant contributions and guidance from Dr Chris Lowe.

Acknowledgements

I have countless people to thank for getting me through and I would not be in the position of writing this thesis without them!

First and foremost, I would like to thank my primary supervisor, Chris. You have been instrumental in helping me to work around the problems, providing constant support and putting up with a bombardment of emails and questions. You have gone above and beyond the supervisory role and set a new benchmark that I hope all MbyRes students have the pleasure to experience. Your calm and collected approach to everything has kept things stable and given great insight when approached with wacky ideas and concepts. I am sure the day this thesis gets submitted will be as great a relief for you as it will be for me!

Secondly, I would like to thank my secondary supervisor Al, in addition to Wiebke, Lenny, Jack, and all the folks that worked in the Animal facility over the last few years. I was blessed to be given the opportunity to work with you all on some interesting research topics, yes Lenny even the endless data entry! The work was so rewarding, especially the undergraduate projects – which were a hoot to design and an absolute pleasure to be involved in. I've always been interested in mirror trials and was ecstatic when the opportunity arose to 'invent' an experiment that utilised them! It certainly helped me design my experiment for the second chapter, and for that I am eternally grateful.

Thirdly I would like to thank Nicole, for your rapid responses to a multitude of issues within the lab during data collection, keen interest in what I was doing, and positive attitude that illuminated the room every time you popped your head around the door!

Finally, I would like to thank friends and family, who were there through thick and thin without hesitation. To the lads - Kingsley, Will and Louis, I cannot thank you enough for coming all the way down for numerous weekends of laughs, sports, and the occasional beer. To my family and Eleanor, you have been immense as always. Without your support and 'constructive criticism' throughout my education, I wouldn't be anywhere close to where I am today. I love all of you dearly, and as you have always said, 'time to look onwards and upwards, and make every day better than the last'.

Thank you all once again, though thanks will never be quite enough after all you have done for me. Time to enjoy some science!

Definitions and Abbreviations

- GFP – Green Fluorescent Protein.
- LED – Light Emitting Diode.
- OS – Open Source.
- PAR – Photosynthetically Active Radiation
- ROS – Reactive Oxygen Species.
- RPi – Raspberry Pi Computer
- SMO – Small Marine Organism.
- UV – Ultraviolet.

General Introduction

Organismal responses to changing environments are key to our understanding of fundamental biological processes and future ecosystem dynamics (Harley *et al*, 2006; Chown *et al*, 2010; Monaco and Helmuth, 2011). Human activity has accelerated environmental change on a global scale, causing direct and indirect damage to the marine environment (Johnson and Hofmann, 2020). For example, overfishing to feed a growing population results in trophic cascades; whilst industrial processes and deforestation emit waste products (such as CO₂ and heavy metals) to the atmosphere and oceans (Taylor and Lloyd, 1992; Bellwood *et al*, 2011; Myriokefalitakis *et al*, 2015). Whilst the long-term ecological impacts of climate change are yet to emerge, short-term ecological impacts such as coral bleaching are causing major concern for our planet's ecological future (Hoegh-Guldberg *et al*, 2017; Trenberth, 2018). Understanding and mitigating these impacts requires detailed insight into the fundamental processes that depend on abiotic stability and act as a foundation for wider biological functions (Andersson *et al*, 2015). The symbiotic associations between cnidarians and unicellular algae are common model systems used to assess the impacts of abiotic variation as a result of their ecological and economic value, and have thus become standards for studying human impacts on the marine environment.

Cnidarian symbioses are essential drivers of production in tropical environments, using both solar energy and particulate organic matter to condense sparse nutrients into tissues that fuel the reef ecosystem. To form the symbiosis, free-swimming dinoflagellates (algae) are absorbed into the corals' (host) tissues by endocytosis, and then displayed within the epithelial cell layer to maximise light and nutrient availability (Davy *et al*, 2012). The resulting intracellular environment encourages photosynthesis and multiplication, increasing symbiotic efficiency. The relationship between cnidarian hosts and symbionts depends on maintaining an equilibrium between symbiont density and photosynthetic output (Decelle, 2013). Abiotic stressors amplify the costs associated with maintaining symbiosis and will lead to a rapid breakdown of the relationship without mitigation by physiological adaptation (Muller-Parker, D'elia, and Cook, 2015). For example, high light intensities promote algal growth, and require selective downregulation of dividing algal cells within host tissue to prevent high densities and consequent nutrient depletion over time (Wooldridge, 2010). Long-term climate change will

cause changes in light intensity and spectrum, creating potentially hostile conditions for photosynthesis in equatorial waters unless rapid adaptation by hosts or symbionts can occur (Cumbo, van Oppen and Baird, 2018).

Adaptation to specific light environments (i.e., intensity and spectrum) by photosymbiotic organisms is diverse but understudied. Cnidarian species are often subcategorised as distinct colour morphs, distinguished by the expression of various fluorescent proteins and other pigments. These proteins are used to enable the cnidarian-algal symbiosis to maximise efficiency in certain light micro-environments by transforming light before it reaches the photosymbionts. For example, some photosymbiotic cnidarians express a green fluorescent protein (GFP) in their epidermis that absorbs harmful ROS-inducing UV radiation (Hansel and Diaz, 2020), and fluoresces a proportion of the energy as photons within the visible spectrum (Salih *et al*, 2000). These GFPs consequently enable certain cnidarian-algal symbioses to operate at high light intensity and light spectrum that is indicative of shallow tropical waters, without incurring cellular damage.

In temperate environments, large coral structures are limited by lower abiotic stability (compared with the tropics) and the cnidarian clade is consequently dominated by hardy sea anemones and jellyfish (Muller-Parker and Davy, 2001). Temperate sea anemones are highly mobile, with complex behaviour in response to abiotic variations as a mechanism to maintain symbiotic balance in variable habitats (Begood *et al*, 2020). Cnidarian behaviour in response to light stimuli (phototaxis) is a topic that has gained interest in recent years, yet fundamental questions remain unanswered. For example, why are GFPs expressed in temperate and low UV environments? Do colour morphs have differing preferences for specific light intensity?

There is a lack of understanding as to why different colour morphs of species associated with GFP expression occupy similar habitats, particularly in temperate environments where UV levels are low. GFP expressing morphs should dominate at high light intensities due to their photoprotective function, yet GFPs are also found at depth which suggests an alternative function (Roth *et al*, 2015, Tsutsui *et al*, 2016, Eyal *et al*, 2015). Individuals are potentially selecting specific light microenvironments throughout the euphotic zone as a result of spectral transformation by GFPs, either by transforming UV radiation into visible wavelengths, or transforming blue-shifted wavelengths into photosynthetically

active radiation (PAR) to increase symbiont efficiency at depth (Smith *et al*, 2017). Temperate light microenvironments are more variable than their tropical counterparts and may favour expressive or non-expressive morphs as short-term conditions change. This would allow morphs of a motile species to reside at similar depths whilst occupying different light microenvironments. The role of GFPs may become less crucial for survival in temperate species and serve as a fitness boosting function dependent on local weather or season. However, this is yet to be studied. These observations suggest that fluorescent proteins such as GFPs, and cnidarian colour polymorphism generally, may play a role beyond photoprotection and constitute more subtle adaptations to differing light microenvironments. Therefore, the physiological or behavioural consequences of GFP expression needs further study.

Respirometers and photo-respirometers are typically designed with particular target species in mind because the size of an organism, and its husbandry requirements, place constraints on their design (Raskoff, 2013). Consequently, commercial systems are available for a relatively modest range of organisms, based on customer demand and commercial viability, and means that the aquatic physiology discipline has a long history of 'home-engineering' involving the modification of equipment or building from scratch. Advances in 3D printing and open source (OS) hardware and software has resulted in greater potential for custom or flexible apparatus design as required by the user. As a result, highly customised prototype equipment can be developed at a fraction of the cost of commercially available kit, which is a particularly desirable approach for early career researchers with limited funds (Fisher and Gould, 2012; Drown *et al*, 2020).

OS technology is derived from the core principle that any person can design and share software or hardware, which can then be freely downloaded and modified. This philosophy has become a major source of innovation and has contributed to rapid technological advances and application in biological sciences. However, there are costs involved when using OS technology. Prototypes and apparatus developed without prior knowledge or experience of specific research applications or techniques may lack the accuracy and precision of commercial systems. It is essential that OS-based research methods are continuously

scrutinized to ensure data collection remains accurate, and that consequent scientific conclusions are valid.

Researchers are beginning to use the OS philosophy across diverse marine disciplines. For example, 'sonic kayaks', and a citizen science approach are being used to collect high spatial resolution sea surface temperature and underwater noise data in coastal environments (Griffiths *et al*, 2017); whereas OS artificial intelligence systems have been developed to investigate vocalisations of marine mammals amidst non-biological and ambient background noise (Thomas *et al*, 2019). In the field of aquatic physiology, there are an increasing number of OS respirometers designed to meet specific applications such as high throughput measurement or portability (Svendsen, Bushnell and Steffensen, 2016; Byrnes *et al*, 2020; Drown *et al*, 2020). However, the number of photo-respirometers for investigating the cnidarian-algae symbiosis in response to varied light intensity remains low, with greater focus for aquatic photo-respirometry on microalgae and macroalgae productivity (Tait and Schiel, 2010; Sánchez-Zurano *et al*, 2020). Our understanding of processes within cnidarian photosymbiosis will benefit from increased accessibility, and OS photo-respirometers are a suitable alternative to commercial systems.

Physiological adaptations often yield behavioural responses that enable organisms to maximise their efficiency within a certain environment. Photosymbiotic cnidarians react to changes in light intensity to maximise photosynthetic efficiency by actively managing the symbiont density within their tissues, and in the case of motile species, moving between and within ideal light microenvironments. As seen before, colour morphs are potentially adapted to maximise efficiency within different light microenvironments, and we would therefore expect to find colour morphs of motile species at distinct depths or within distinct microhabitats. In temperate motile species of sea anemone, this is not always the case as morphs seem to occupy similar depth distributions despite being subcategorised by their GFP expression. Motile behaviour in response to light intensity (phototaxis) has previously been investigated in temperate sea anemones in response to varied spectral composition (Foo *et al*, 2019), but has not focussed on the behavioural differences between colour morphs of the same cnidarian species (with common symbionts). Investigating behavioural differences between morphs will enable a holistic understanding of the functional

roles of both GFP expression in temperate species and general cnidarian colour polymorphism and reduce the current gap in our understanding of this important aspect of cnidarian-algae photosymbiosis.

In the following two chapters, the physiological and behavioural adaptations of colour morphs within the Snakelocks anemone (*A. viridis*, or sometimes known as *A. sulcata*) – *Symbiodinium* symbiosis will be investigated. Individuals are polymorphic dependent on their GFP expression, yet the functional roles of GFPs and consequent anemone behaviour in response to light is poorly understood (Mallien *et al*, 2017; Porro *et al*, 2020). This study species will address the two challenges presented in this introduction: making metabolic research more accessible and diverse, and furthering our understanding of GFP functional roles within the cnidarian-algae symbiosis. Chapter 1 describes an OS-inspired photo-respirometer that shows capability in designing and modifying apparatus for metabolic research whilst retaining accurate and precise data collection on intricate biological processes. This will be beneficial to large scale investigations into factors that affect metabolism in SMOs and exemplifies the potential application of such OS apparatus in higher level research and teaching. Chapter 2 explores the behavioural responses of *A. viridis* to varied light intensity, which has not previously been investigated in detail. Polymorphic variation in response to light intensity may present a new perspective on the functional roles of GFPs within the *A. viridis* – *Symbiodinium* symbiosis. Consequently, the extent of behavioural differences between colour morphs may enable more accurate predictions of the general responses of cnidarian-algal photosymbioses to changing environments and may ultimately inform the design and execution of effective management strategies in protecting this photosymbiosis for the future.

Chapter 1 – Open Source Respirometry: A Low-Cost, Versatile Apparatus for Collecting Metabolic Data on Small Marine Organisms

Matthew J. Kyle-Henney, Valentina Balzarini, Daniel Martin, Alastair J. Wilson
and Chris D. Lowe.

University of Exeter, Centre for Ecology and Conservation, College of Life and
Environmental Sciences, Penryn Campus, Cornwall, TR10 9FE, UK.

Abstract

Respirometry is a key topic for studying the ecology of aquatic organisms, yet limitations in the complexity and resulting cost of commercial apparatus make aquatic respirometry relatively inaccessible to many early career researchers. Alternative open source systems have become increasingly common in biological sciences due to their ease of design, manufacture, and modification, yet there is a gap in open source designs for investigating metabolism in small marine organisms. This study describes an alternative, open source photo-respirometer for measuring photosynthetic and respiration rates in sea anemones, that can easily be modified for other target organisms and research topics. The simple modular design addresses the key limitations of respirometry in general, without losing accuracy or precision in data collection. Metabolic rates of two colour morphs within the *A. viridis* – *Symbiodinium* photosymbiosis in response to varied light intensity were used to exemplify the photo-respirometer's data collection capability. Green morphs express green fluorescent proteins (GFPs) whilst brown morphs are non-expressive. The results of the example study found that metabolic rates did not differ between morphs and were not influenced by acclimation condition. Open source systems, such as this photo-respirometer, are capable of collecting reliable data for use in many aspects of aquatic biology, and may be suitable for fundamental research across multiple disciplines.

Introduction

The characterisation of metabolic rates is a cornerstone of a variety of ecological and physiological disciplines. For aquatic organisms, major metabolic processes such as respiration and photosynthesis are often quantified as oxygen consumption or production over time. Measurement of metabolic rates often involves housing subject animals, plants, or algae in enclosed containers, such that oxygen flux in the water can be used as a proxy for organismal metabolism. Such systems allow the effect of various physical stressors, such as temperature and pH, on metabolic rates to be assessed and are thus an important approach in understanding abiotic impacts on marine systems.

Whilst in principle respirometry is simple, the precise and accurate measurement of metabolic rates is fraught with challenges. For example, the characteristics of oxygen electrodes and sensors, the requirement to control environmental factors (such as temperature and light), and the characteristics and behaviours of the subject organisms themselves, all impose specific requirements and design challenges on respirometry equipment (Rodgers *et al*, 2016; Svendsen *et al*, 2015; Steffensen, 1989). As a result, whilst a variety of commercial respirometers and photo-respirometers are available, aquatic physiology has a long history of making and customising laboratory equipment. In recent years, the increasing availability of cheap microcomputers, 3D-printing, and OS sharing of software and hardware has further driven the development of customised laboratory equipment (Hope, 2008; Sherpa *et al*, 2017; Deek and McHugh, 2007). Converting a commercial respirometer requires considerable thought, planning, prototypes, material, and thus induces high cost. Alternative OS apparatus designs can be downloaded for free and are modular to ease fitting. Additionally, access to 3D printing is becoming common in research facilities (Pearce, 2012), which allows researchers to quickly modify and refine designs without the need to buy expensive replacement parts.

In the study reported here we used the OS idea to develop a low-cost aquatic photo-respirometer for the measurement of metabolic rates in symbiotic sea anemones, that could also provide a platform for modification to measure other small marine organisms (SMOs). The physiological responses of cnidarian-algal symbioses (such as corals and anemones) are a major focus for researchers aiming to understand the impacts of environmental change on coral reefs

(Fransolet *et al*, 2012, Fulra *et al*, 2011). Whilst tropical corals and anemones are most vulnerable to environmental change, temperate cnidaria-algal photo-symbioses also occur and many are used as tractable models to understand the broader physiological mechanisms that underpin photo-symbioses (Lehnert *et al*, 2012, Verde and McCloskey, 2007). With some basic skills in electronics, 3D-printing, and programming the system is simple to build and cost-effective.

We initially used two individuals of the Snakelocks anemone (*A. viridis*, or sometimes known as *A. sulcata*) as example SMOs to show the raw data output of the photo-respirometer, and then tested the design's capabilities when investigating complex hypotheses. We used the temperate cnidaria-algal photo-symbiosis between *A. viridis* and *Symbiodinium* to investigate the currently unknown primary roles of temperate green fluorescent proteins (GFPs) on enhancing photosynthetic responses to varied light intensity. Whilst we developed the equipment with a specific target organism in mind, the system could easily be modified to accommodate other subjects and we hope that the system provides a platform on which others may expand.

Materials and Methods

The Subject Organisms – photosymbiotic cnidaria

Our motivation for developing an aquatic photo-respirometer was to examine the physiological responses of *A. viridis* and their *Symbiodinium* algal partners, particularly the responses of two colour morphs that are expressive (green morph) and non-expressive (brown morph) for GFPs.

In corals, GFPs have photoprotective and transformative roles, enabling symbionts to maximise their photosynthetic efficiency under high light stress – such as high UV radiation and intense, blue-shifted spectrum. These primary roles of GFPs are useful in tropical environments. However, their primary roles in temperate environments are unknown, as these environments are highly variable in terms of light intensity but have lower levels of UV radiation and a shallower euphotic zone than in the tropics. We would expect that temperate GFPs have a benefit in terms of photosynthetic efficiency at high light intensity, which may be influenced by the host's reliance on the symbiosis for energy (Salih *et al*, 2000; Dove *et al*, 2001). To investigate the primary roles of temperate GFPs, we acclimated 4 groups containing both morphs of *A. viridis* to high or low light

intensity and high or low food availability. We hypothesised that green morphs would exhibit greater photosynthetic responses than brown morphs as a result of their GFP expression; and that differences between morphs would vary due to heterotrophic energy availability.

Design Overview

Our primary aim was to design a system to measure respiration and photosynthesis in photo-symbiotic sea anemones. While photo-respirometers are commercially available (eg: Hansatech oxylab, Qubit systems OX1LP) these have small measurement chambers (1-50ml), and thus were an order of magnitude too small for our purpose. In addition to this minimum size constraint, the commercial systems can lack a temperature control device, a mechanism for delivering actinic light (to drive photosynthesis) or exclude light entirely (to measure respiration), and the flexibility to operate as a closed or open cell respirometer with continuous or intermittent flow (to adjust the sensitivity of the system and to maintain normoxic conditions for the purpose of animal welfare). Consequently, our system had to meet four major system requirements: water-tight housings and a system for circulating water and controlling temperature, light delivery and control, an integrated oxygen probe/detection system, and a control system with a user interface. Whilst the majority of the system is custom made, we used a calibrated PreSens Fibox oxygen detection system based on non-invasive quenching sensor dots, although a variety of different sensor types could easily be incorporated in the system we outline.

System Components

Housing and Circulation - The 'wet components' of the respirometer consisted of three chambers: one to house the oxygen sensor, one to house the subject organism (subject chamber), and a reservoir to replenish the water in the system (Figure 1). The oxygen sensor was placed in a separate chamber to the subject organism because quenching sensors are strongly affected by high light intensities, and a separate chamber allowed either intermittent or continuous water flow as required. During testing, we also found that contact between the subject organism and the sensor disrupted the output signal. Thus a separate housing for the oxygen sensor fulfilled several important requirements.

For the measurement and reservoir chambers we used standard Durian bottles with tri-port lids, which allowed the system to be easily plumbed together. The subject chamber was a 500ml, water-jacketed beaker. Temperature control was achieved by circulating water from an electronic water bath through the jacket. Submerging the subject chamber in a water bath (a common approach for aquatic respirometers) was ruled out since this complicates arrangements for providing light to drive photosynthesis. We manufactured a custom 3D printed lid, fitted with 3 nitrile O-rings to seal the chamber, and a screw thread compatible with the Duran tri-port lid for connection to the rest of the system. The chambers were interconnected with a series of oxygen impermeable 6mm Viton tubes and circulation was generated via two peristaltic pumps (Williamsons 200xc). Each tube was wrapped in a neoprene sleeve to maintain temperature. The system was arranged so that water either circulated between the subject and measurement chambers (during a measurement phase) or from the reservoir, through both chambers, and back (during a rest/recirculation phase).

Light Delivery – The clear subject chamber allowed us to mount a lighting rig directly on the beaker. We used three 50 Watt, full-spectrum (visible not UV) white LEDs (TruOpto) to drive photosynthesis. LEDs were housed in a custom 3D printed shroud that fits over the subject chamber (Figure 2, technical drawing in Appendix Figure A1). The LEDs were mounted on heat sinks backed by 12V CPU fans to dissipate excess heat away from the subject chamber and maintain stable temperatures within the chamber. In addition to LED positioning, the shroud provided some protection for the LEDs from water splashes and acted as a barrier to surrounding ambient light (closed cell foam was used to further insulate the subject chamber and to completely block ambient light). The entire hardware setup for the respirometer can be assembled on a standard laboratory desk (Figure 3).

Control System and User Interface – The basis of the control system was a Raspberry Pi 3 microcomputer (RPi). The wiring layout and components are detailed in the Appendix and a brief description is provided here. The RPi was used to control the LED output, cooling fans and peristaltic pumps via the built-in GPIO input and output pins (Table A1). Pumps and cooling fans were connected to a 12V 4 channel relay (one channel was left unused) and controlled via the standard RPi GPIO utility. LEDs were each connected to a 3 channel Picobuck

LED driver (see Appendix) and their output controlled via pulse width modulation (using the Pi-blaster software: <https://github.com/sarfata/pi-blaster/>).

We controlled/coordinated the system components using an R shiny app (Chang *et al*, 2020) running on a laptop PC. We elected for this option rather than a web server hosted on the RPi for three reasons: firstly, the processing capacity of the RPi is relatively limited; secondly, our chosen oxygen detection system required a PC in any case; and thirdly, R is a commonly used language for processing and analysing data in biological sciences (making the app simple to integrate with downstream analysis). The basic function of the app was to relay user commands to the RPi (using the SSH communication protocol), to display oxygen concentration data generated by the Fibox sensor, and to integrate the oxygen data with light intensity settings during Photosynthesis-Irradiance (PI) curve measurements. We opted for the SSH communication protocol, due to our familiarity with Linux, which was facilitated on the PC using the Cygwin utility. SSH security keys were set so that each SSH command could be transmitted without requiring a password interrupt and therefore limit SSH delay. Operating the photo-respirometer requires the setup of SSH keys between the user's laptop PC and the RPi, which requires little knowledge of software programming. Running the shiny app in Rstudio will then automate communication between the laptop PC and the RPi and begin to collect measurements.

The shiny app provides manual control of each system component, and a programmable PI curve which allows the user to define a series of light steps to control the time period over which a metabolic rate is measured. The user can also define a recirculation period at the start of each light step, which serves as a brief acclimation (typical of PI curve measurements) and during which the water in the system is replenished to normalise oxygen concentrations. We did not attempt to integrate control of the Fibox system into the shiny app as it was beyond our programming ability. Consequently, the current system's proprietary Presens software must be run alongside the app. However, once recording is started, the shiny app reads the log file and displays the oxygen flux data and current light level to allow monitoring of the experiment. The app also generates a data file in real time in which the oxygen flux data, light intensities, and measurement periods are integrated ready for subsequent analysis.

System Testing – Figure 4 shows examples of oxygen fluxes during the measurement of photosynthesis-irradiance (PI) curves in *A. viridis*. These curves show oxygen flux over time, indicating the rate of photosynthesis and/or respiration, for multiple light intensity increments. We used this example to showcase the capability of our photo-respirometer in context.

PI curves were initially produced for individuals of each morph, with changes in light intensity occurring at set times during the measurement phases and separated by recirculation phases of the experiment. We adjusted the raw data curves for brown and green individuals with ‘short’ (light intensity from 0 to 400 $\mu\text{mol photons/m}^2/\text{S}$) and ‘long’ (light intensity from 0 to 1000 $\mu\text{mol photons/m}^2/\text{S}$) experiment lengths, and a ‘Blank’ response for measuring background flux without an anemone subject (Figure 4). Literature has noted the importance of mitigating background respiration in respirometer design, and must be considered (Rodgers *et al*, 2016). In our design, we minimised the length of tubing and flushed the system with 1% Milton fluid between each experiment to sterilise all internal surfaces. We tested water from the anemones’ holding tank, shown as the ‘Blank’ responses. We determined that the level of background microbial respiration within the system was negligible as the rate of oxygen flux was 0 $\mu\text{mol/L}$ (± 0.05). The recirculation and measurement phases were isolated using a processing function. The rate of photosynthesis could then be calculated by the change in oxygen concentration over time using linear modelling.

GFP Example Investigation – Comparisons of photosynthetic rates between individuals can determine the photosynthetic efficiency of a population and observe variation between morphs with individual level random effects. For the analysis of GFP effects on photosynthetic rates, we collected a similar dataset to that of figure 4 from 35 individuals acclimated to two light intensity conditions and two feeding regimes – creating 4 acclimation groups for each morph. These groups consisted of high light intensity and high food availability (HLHF), high intensity and low food (HLLF), low intensity and high food (LLHF) and low intensity and low food (LLLLF). We converted the raw PI data into photosynthetic rate plots to showcase our photo-respirometer’s capability for complex hypotheses (Figure 5). We fitted the Eiler’s PI curve model (Eilers and Peeters, 1988) using the nls model analysis in Rstudio to predict and therefore smooth the individual photosynthetic rates. This model follows a saturating curve pattern,

from which photosynthetic efficiency (a), photosynthetic maxima (P_{max}), and optimal light intensity (I_{opt}) could be assessed (Figure 6).

Results

At first glance, brown morphs appear to have greater average photosynthetic rates than green morphs when acclimated to HLLF, and morphs do not differ in average photosynthetic rates when acclimated to the other conditions (Figure 5). However, Kruskal Wallance tests were conducted on the parameters created by the Eilers model, and found no significant differences ($p > 0.05$) between groups for 'Pmax' ($H(7) = 8.16$, $p = 0.319$), 'Iopt' ($H(7) = 9.85$, $p = 0.197$), or 'a' ($H(7) = 5.51$, $p = 0.598$). Parameter 'c' was normally distributed and tested using analysis of variance, however differences between groups were also non-significant ($F(7) = 2.18$, $p = 0.0682$). These results show that the visual difference between the average responses of brown and green morphs was not significantly different, and that neither morph nor acclimation condition influenced photosynthetic responses between groups.

Discussion/Conclusion

As technology advances, OS systems will be upgraded and modified to answer a diverse range of biological research. There is clear potential for OS systems to become the mainstay in small scale laboratory research, particularly in postgraduate research applications where targeted modification would enable a deeper understanding of key biological processes without access to large research grants. The aquatic photo-respirometer described in this paper has a simple design that acts as an ideal platform for modification and remains cost-effective. However, for use in research contexts, the apparatus must be able to obtain accurate, reliable data. The algae-cnidarian symbiosis example showcased both the capability and adaptability of the respirometer's design. The lack of background flux during the 'blank' responses indicates a high level of accuracy whilst the linearity in measurement phase responses indicates high degree of precision. This enables confidence in the system when drawing conclusions about the *A. viridis* – *Symbiodinium* symbiosis.

The results of our example investigation do not show significant variation between morphs or acclimation groups. There may be several theories as to why morphs do not differ in their photosynthetic responses to varied light intensity that

contradicts the primary roles of GFPs in other photosymbiotic cnidaria and should be explored further in the future. Under HLLF conditions, brown morphs may potentially have higher relative photosynthetic rates at all light intensities than green morphs, but a larger sample size and more direct hypotheses may prove this with statistical significance. This research may be pivotal to our understanding of the cnidarian-algae symbiosis, as potential variation between morphs that produce fluorescent proteins could predict both the impact of physical stressors on shallow water ecology, and the response of shallow water organisms after a major stress event such as bleaching (Aihara *et al*, 2019). Alternatively, no variation between morphs, as seen in this investigation, may hint at secondary roles of GFPs such as prey attraction (Haddock and Dunn, 2015) that does not influence photosynthetic rates. The testing and results produced by our photo-respirometer show the design's capabilities for investigation into compelling relationships within marine photosymbioses, further proving its worth for use in current metabolic research.

Despite this, there are areas where the design could be improved. Firstly, removing the sensor from the subject chamber and into a separate measuring chamber increases apparatus volume. This increases the surface area for bacterial growth, which in turn increases background respiration within the system. Reducing the length of circulation hoses and other non-essential surface area mitigates the issue. Noise caused by background respiration can be calibrated for: however, accuracy is increased when the background respiration is already minimal. Secondly, the parameter estimates of I_{opt} in Figure 6 suggest that light intensity should be increased to reduce excessive extrapolation during analysis. This may require simple code change to increase the intensity of light per LED or may require brighter LEDs that would need rewiring. Finally, the modular design makes the apparatus easy to disassemble for cleaning, but the independent components make the collective system awkward to move. It would be beneficial to mount the apparatus in a way that reduces space and increases manoeuvrability. Whilst this is not a major requirement, it would enhance the potential for undergraduate teaching applications and will be beneficial in shared laboratories that are space limited.

It is worth noting that motile organisms, such as fish, may require continuous water flow that elevates the respirometer's complexity. A flume-style chamber

could be interchanged for the subject chamber (in our design), whilst utilising the other core components of the system. For small fish, the intermittent flow system could be refined by setting a minimum oxygen concentration limit within the subject chamber, that triggers a chamber flush to replenish oxygen in the case of user error. This would conform with the 3Rs in the case of vertebrate welfare, in addition to larger chambers that allow the mobile organisms to move naturally. This adaptability would allow researchers to explore broader questions within metabolic study of small organisms, further highlighting the value of customisable OS designs.

In conclusion, the described respirometer design is an ideal candidate for alternative apparatus in biological research, with vast potential in research and teaching contexts whilst maintaining the OS system criteria. Whilst the respirometer is a relatively specific apparatus for measuring metabolic rates in marine organisms, relative performance against commercial apparatus should prove the viability of OS systems as alternatives for most aspects of biological data collection.

Figures

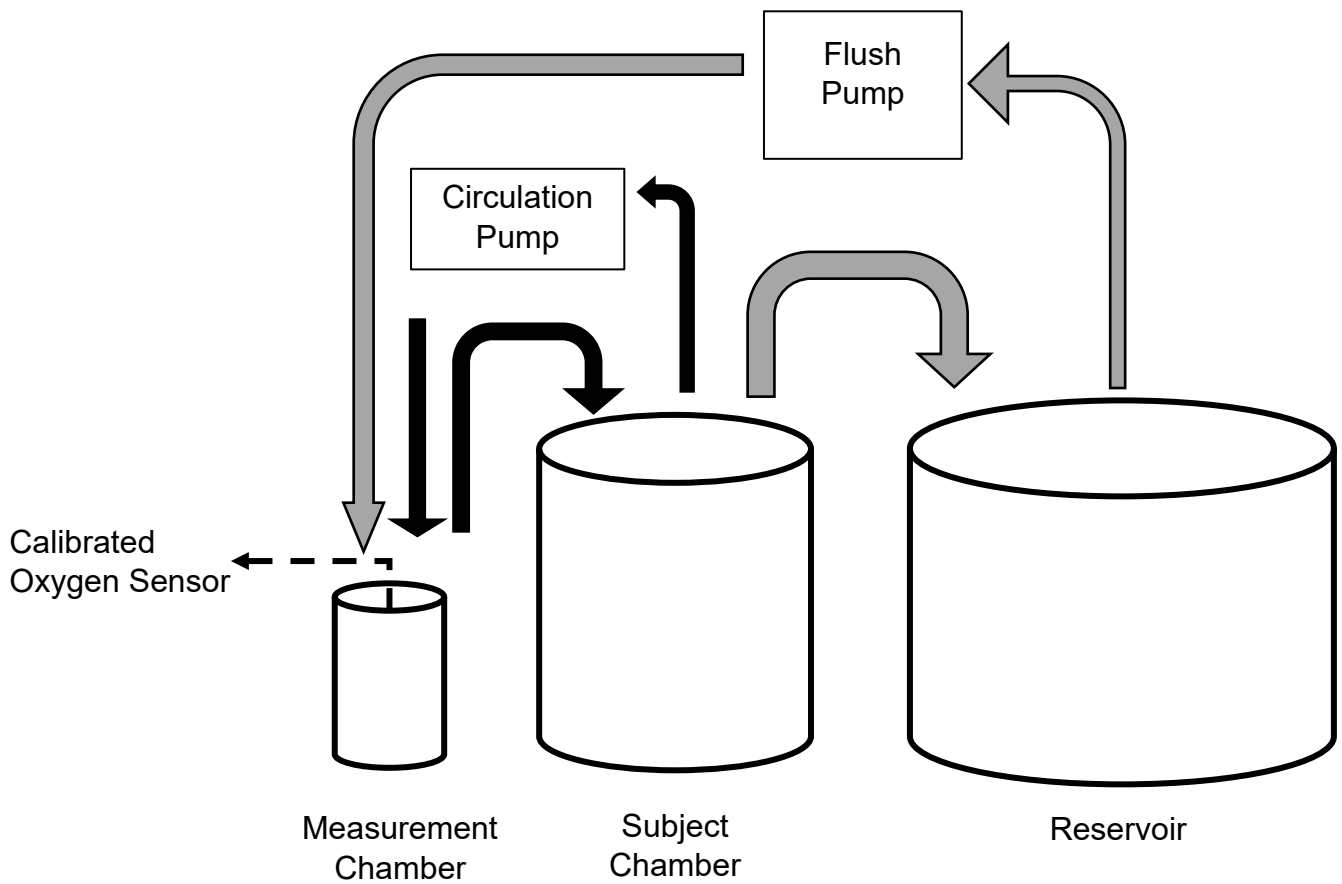


Figure 1: The basic layout of the respirometry system. The circulation pump provides constant water flow (black arrows) between the subject and measurement chambers during measurement phases. The flush pump controls water flow (grey arrows) between all chambers to replenish oxygen concentrations during rest/replenish phases. The oxygen sensor in the measurement chamber feeds information to the external datalogging system.



Figure 2: The LED housing that shrouds the subject chamber and converts the respirometer into a photo-respirometer. LEDs with sunlight-mimicking emission spectra project PAR at the subject from all sides and are cooled by metal heatsinks and electronic fans located in the 3 rectangular sections.

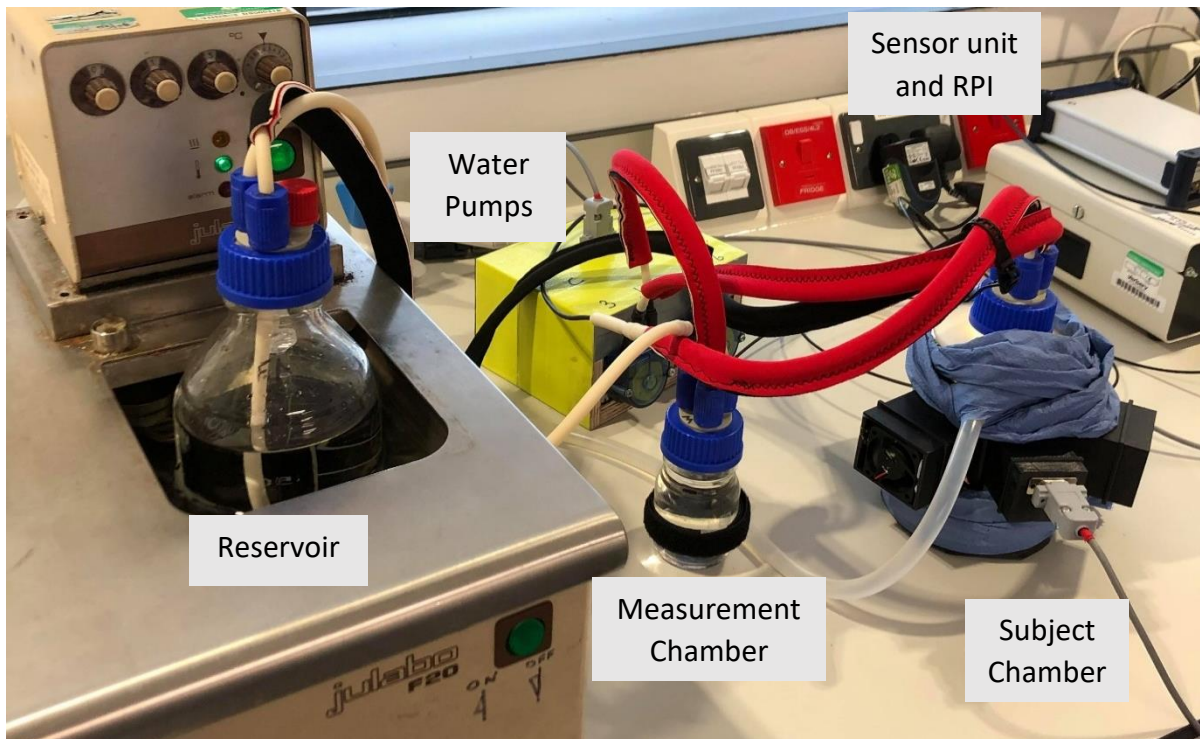


Figure 3: The full photo-respirometer system, including (from left to right): temperature regulating bath containing the reservoir; peristaltic water pumps (yellow box); small measurement chamber containing the oxygen sensor; subject chamber, with blue paper towel to eliminate any external light sources and lighting rig; and the oxygen sensor unit and RPi computer.

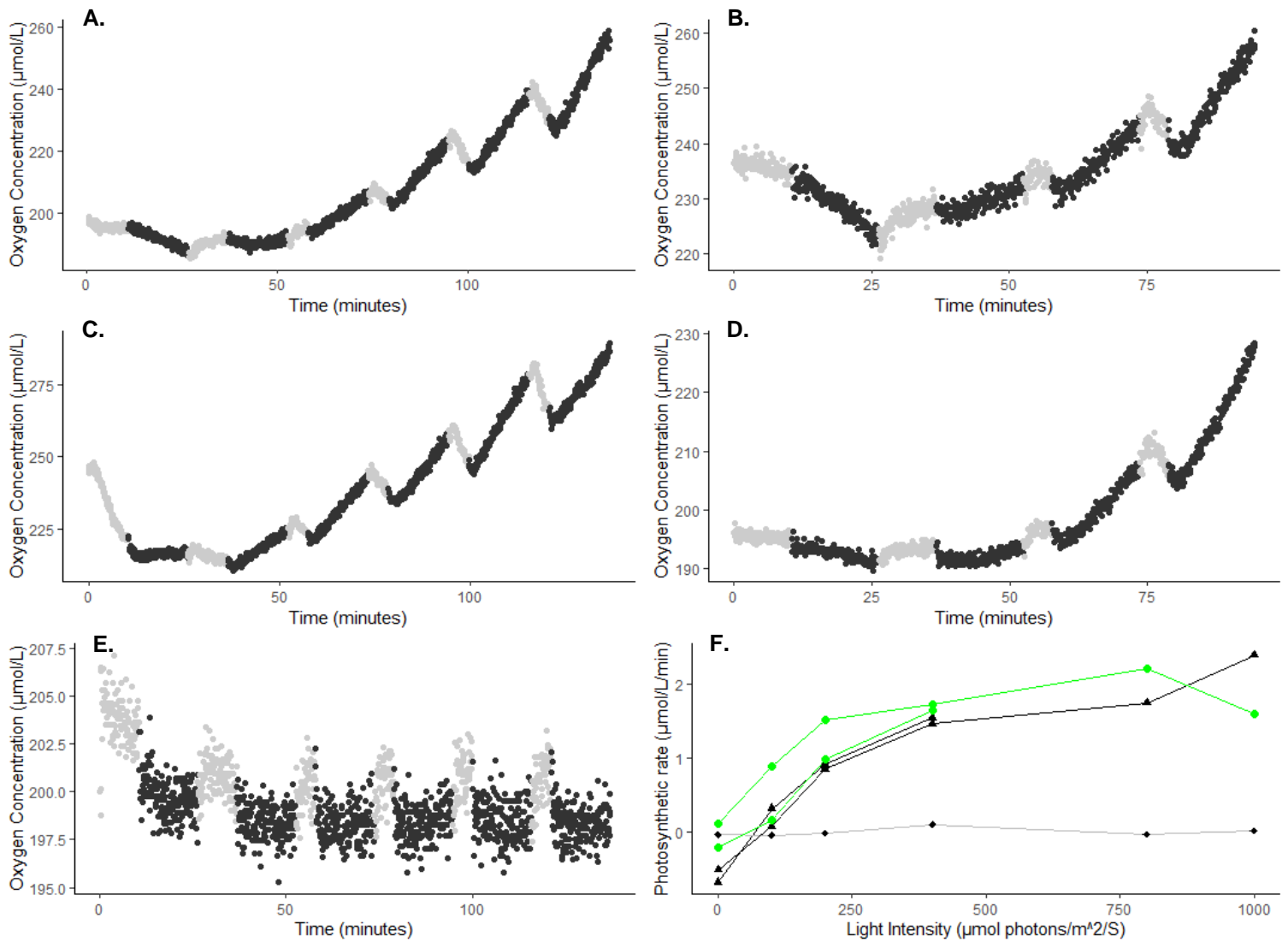


Figure 4: Raw data produced by our photo-respirometer, showing the change in oxygen concentration ($\mu\text{mol/L}$) over time (minutes) for two individual anemones and a control with no individual, and the associated PI curves. Specifically, **A.** shows the photosynthetic responses of a brown morph exposed to a full experimental period with 6 measurement phases, and **B.** shows the same individual exposed to a shorter measurement period. **C.** shows the responses of a green morph exposed to a full period, and **D.** shows the same green morph exposed to a shorter period. **E.** shows the change in oxygen concentration within the system with no individual in the subject chamber as a control for background flux. Light intensity was increased periodically and sustained for 10 minutes at a time, depicted by the black measurement phases, and oxygen concentration fluctuated during the grey recirculation phase as fresh water flushed the subject and measurement chambers (**A. – E.**).

Linear models were used to determine photosynthetic rates during the measurement phases for both individuals and the control, and plotted against the corresponding light intensity ($\mu\text{mol photons/m}^2/\text{S}$) at each phase (**F.**). Black lines with triangular points represent the brown morph (in **A.** and **B.**), green lines with circular points represent the green morph (in **C.** and **D.**), and the grey line with square points represents the control 'blank' response (in **E.**). The gradient of the PI curves can be used to calculate photosynthetic efficiency.

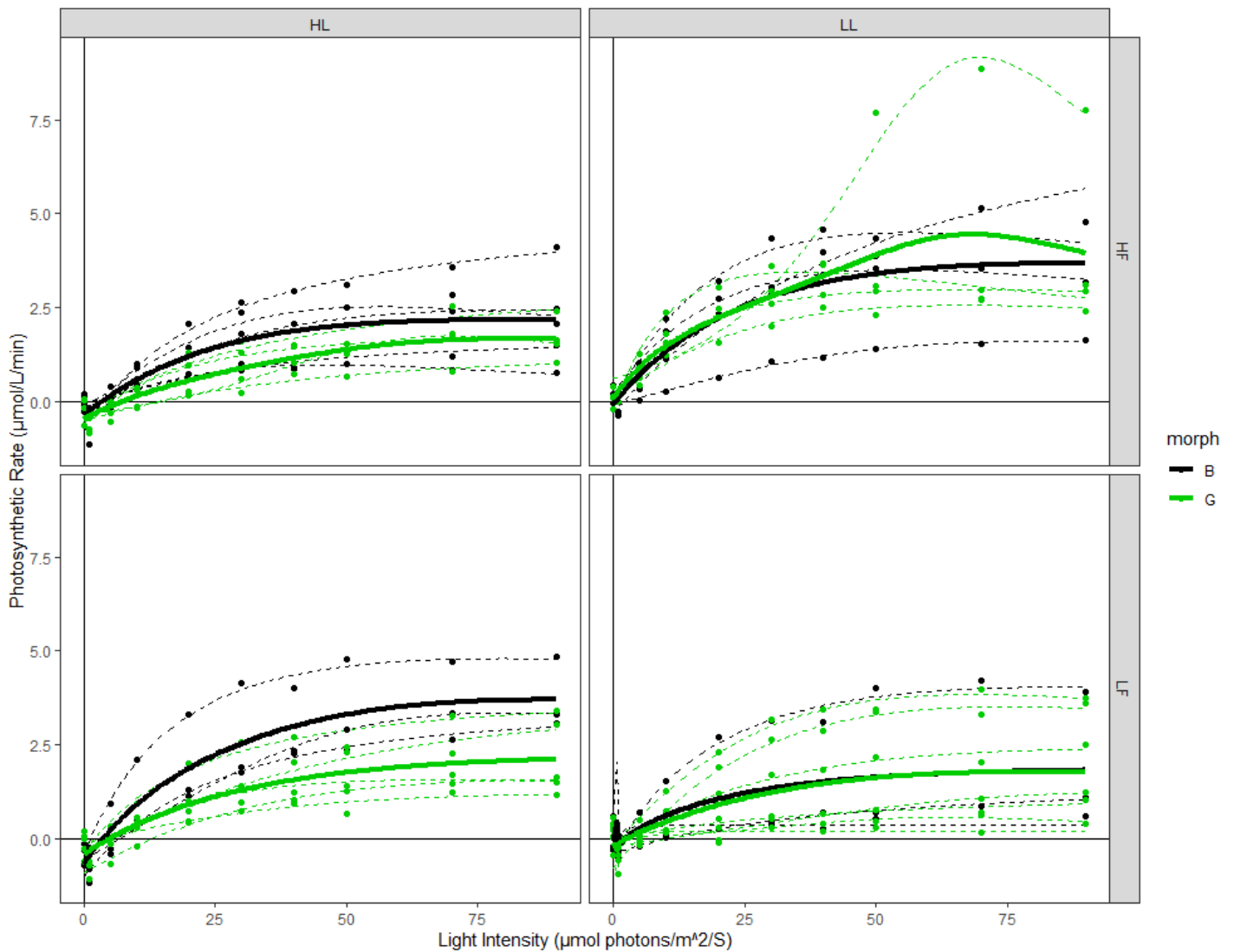


Figure 5: The relationship between photosynthetic rate (µmol/L/min) and light intensity (µmol photons/m²/S) for Brown (black) and Green (green) morphs that were acclimated to 4 conditions: high light and high food (HLHF), high light and low food (HLLF), low light and high food (LLHF), and low light and low food (LLLF). Individual responses are represented by points and model fits represented by dashed lines. Mean responses for brown (black) and green (green) morphs under each condition are represented by thicker solid lines.

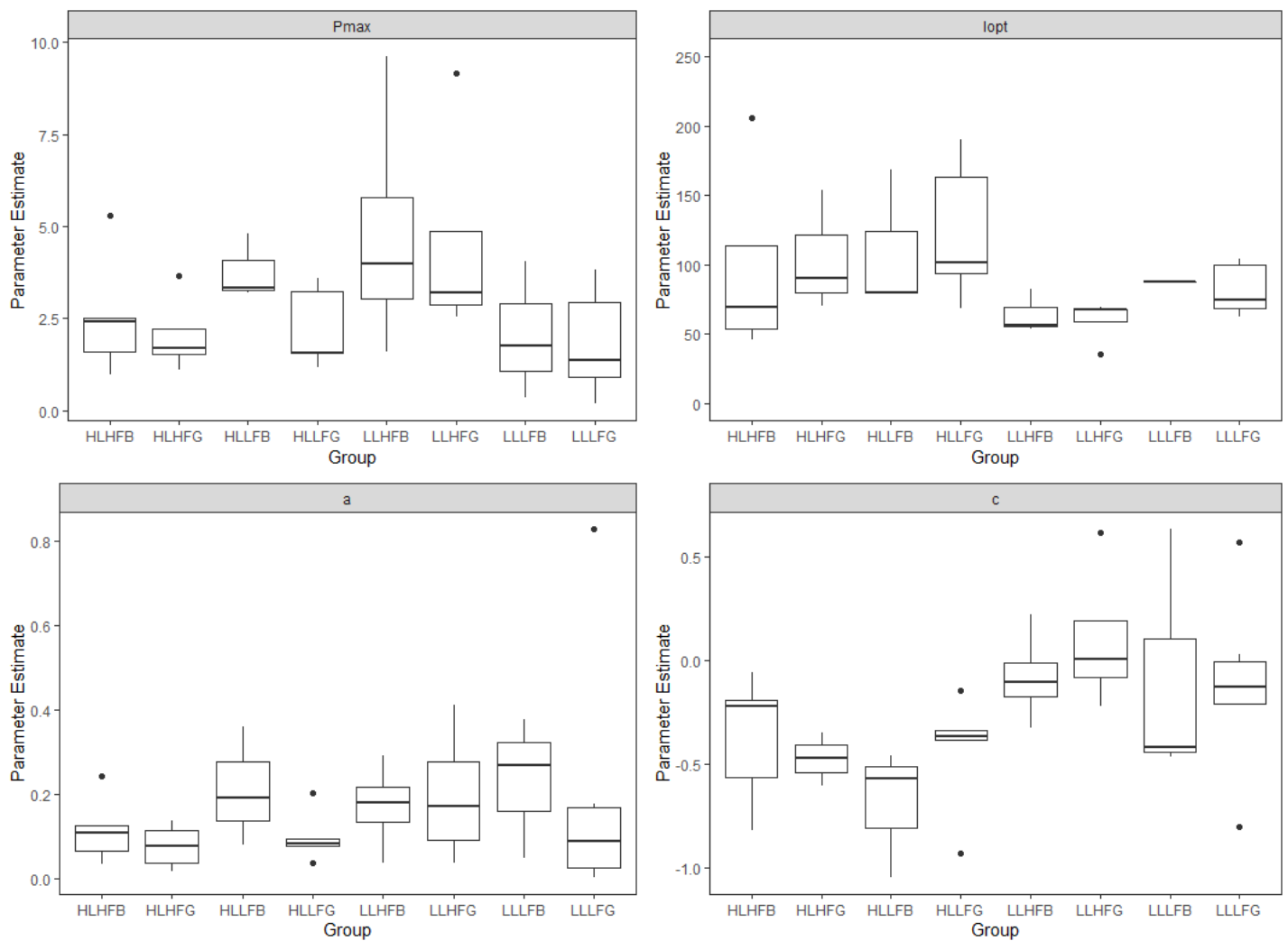


Figure 6: The parameter estimates of the Eilers PI curve model fitted to each group (including acclimation to high or low light, high or low food availability, and morph) within the example investigation data. The parameter 'Pmax' represents the photosynthetic maxima, 'lopt' represents the optimal light intensity, 'a' represents the predicted initial slope of the PI curve, and 'c' represents the y intercept. It is important to note that values in lopt are extrapolated, and some data was excluded from the plot as they lay outside an estimate value of 1000 (particularly in LLLFB). This can be rectified by increasing the value of light intensity during the measurement phases to cause photoinhibition, which would reduce the rate of photosynthesis from the optimal value and prevent excessive extrapolation by the non-linear model.

**Chapter 2 – Phototaxis Behaviour in *Anemonia viridis*: Is
Movement Influenced by GFP Expression and Acclimation
Condition?**

Matthew J. Kyle-Henney, Alastair J. Wilson and Chris D. Lowe.

University of Exeter, Centre for Ecology and Conservation, College of Life and
Environmental Sciences, Penryn Campus, Cornwall, TR10 9FE, UK.

Abstract

Cnidarian colour polymorphism is underpinned by expression of fluorescent proteins, thought to aid photosynthesis under varying light conditions. Green fluorescent protein (GFP) expression provides photoprotection from high light intensity and UV radiation in the tropics, however their primary role in temperate environments remains unclear. This study compared phototactic behaviours of GFP expressive and non-expressive morphs of *A. viridis* in response to a light intensity gradient to determine whether GFP expression provides a photoenhancing function. Theory suggests that morphs should differ in their final position in relation to a light intensity gradient over time, but has not been investigated in this species. The results of this study show that *A. viridis* fundamentally exhibit phototaxis, but this behaviour does not differ between morphs and therefore is not influenced by GFP expression. However, acclimation to low light intensity conditions yielded greater phototactic responses than acclimation to high light intensity conditions, suggesting that symbiont load is the main driver of phototactic behaviour in this temperate photosymbiosis. Interestingly, water flow direction and/or an oxygen gradient may have influenced phototactic responses, which suggests that phototaxis is a behavioural response to both light intensity and oxygen concentration (either directly or as a consequence of water flow).

Introduction

Coastal habitats rely on photosynthetic organisms to fix nutrients into organic matter and fuel ecosystems (Philippart *et al*, 2000). Cnidarian-algae symbioses can make important contributions to this productivity, given their ability to concentrate nutrients in otherwise desolate environments which often leads to diverse reef habitats (Cowen, 1988; Dubinsky and Jokiel, 1994). These symbioses are intricate and sometimes require stable conditions to avoid phase shifts to macro-algae dominance of habitats (Johannes *et al*, 1983). For instance, warming temperatures over time on a global scale contribute to photoinhibition and bleaching in corals that can ultimately lead to overgrowth of macro algae, which in turn results in a loss of biodiversity through trophic cascades. However, cnidarian-algae symbioses must also cope with short term and or local variation in environmental factors. Given its direct impacts on photosynthetic rates and nutrient transfer within the symbiosis, light represents an obvious example of such a factor (Steele, 1976; Muller-Parker and Davy, 2001). Relative to other environmental factors such as temperature and pH, there has been comparatively little research into how, when and why changes in light intensity act as abiotic stressors to photosymbioses. Nevertheless, there is some evidence that photosymbiotic cnidarians exhibit putatively adaptive physiological and behavioural responses to varied light conditions; with fluorescence, symbiont density regulation, and phototaxis being the major focal points for current research. Here we used the Snakelocks anemone (*A. viridis*, or sometimes known as *A. sulcata*) as a model temperate cnidarian to examine phototaxis behaviour as a result of physiological differences between polymorphs.

It is widely hypothesised that adaptation to light intensity environments may explain cnidarian biodiversity (Huston, 1985). For instance, many species of photosymbiotic anthozoan cnidarians (corals, anemones, etc) are polymorphic. Mechanistically, these morphs are differentiated by variations or absences of particular green fluorescent proteins (GFPs) in their epidermal cell layer (Dove, Hoegh-Guildberg, and Ranganathan, 2001; Mallien *et al*, 2017). Functionally, the primary role of these diverse proteins within the symbiosis is debated (Tsutsui *et al*, 2016) as GFPs are thought to both (i) convert harmful UV radiation into blue-green photons before it reaches photosymbionts (Mantha, Johnson, and Day, 2001) , and (ii) alter internal light environments by transforming spectral

properties of light entering the protein to enhance photosynthesis (Smith *et al*, 2007).

These functions are useful in shallow water environments where light intensities may exceed photosynthetic thresholds, causing photoinhibition. In this context GFPs can provide a 'screening' function by transforming excessive light stress (such as high light intensities and UV radiation) to protect the algal symbionts from cellular damage (Salih *et al*, 2000; Smith *et al*, 2013). Some deep-water corals utilise similar GFP wavelength transformation properties to increase the efficiency of their *Symbiodinium* partners at depth, specifically, by transforming a blue-shifted light spectrum into photosynthetically active radiation to aid photosynthesis towards the limits of the euphotic zone (Smith *et al*, 2017). Meanwhile, other heterotrophic cnidarians such as the hydromedusa *Olindias formosus* express GFPs without photosymbiotic associations, where the protein's primary role is thought to actively lure prey items (Haddock and Dunn, 2015). Since some cnidarians are both photosymbiotic and heterotrophic (such as sea anemones) it seems likely that both the photoprotective and prey attractive functions of GFPs may be important.

Alongside physiological adaptations, cnidarians have evolved phototactic behavioural responses. In particular, while adult anthozoans are often viewed as sessile and limited to specific settlement sites, many species are motile and will alter their position in response to light conditions (Pearce, 1974). It is less clear how photosymbiotic cnidarians (and other photosymbiotic organisms) respond to light intensity, be that directly through the use of eyespots or photoreceptors (Picciani *et al*, 2018) or potentially indirectly by photosymbiotic cues (Petrou, Ralph and Nielsen, 2017), as this varies among species. For example, aposymbiotic (bleached by housing in darkness to force symbiont expulsion) Fungiidae corals show phototaxis (Yamashiro and Nishihara, 1995), whereas aposymbiotic sea anemones do not show phototaxis (Foo *et al*, 2019). Determination of the role that intersymbiotic cues play on photo-sensing can be investigated using light intensity acclimation approaches that alter symbiont density within cnidarian-algal symbioses, and therefore alters the magnitude of potential symbiont-to-host signals (Cohen and Dubinsky, 2015). To date, no studies have directly tested for co-variation of GFP morph type with phototactic behaviour within cnidarian species. This is an important omission since, if both

morph diversity and behavioural responses have evolved to enable cnidarians to tolerate, and/or exploit, variable light intensities, we would expect them to coevolve. Natural selection should favour combinations of GFP and behavioural phenotypes such that phototactic behaviour will differ among morphs. Here, we test this prediction using *A. viridis* as a model for GFP-polymorphic cnidarian-algal symbioses.

A. viridis is a common intertidal species found in temperate coastal environments from the Mediterranean Sea to British coastlines. They harbour algal symbionts (*Symbiodinium*), and exhibit colour polymorphism associated with the expression of GFPs. This species has been subcategorised into 5 morphs: var. *rustica*, *smaragdina*, *rufescens*, *viridis*, and *vulgaris* (Forskal, 1775; Mallien *et al*, 2017; Porro *et al*, 2020), although the genetic relationships between (and distinctiveness of) these morphs remains unclear. Along Cornish coastlines, var. *rustica* (brown morph) and var. *smaragdina* (green morph) are the most common forms. Although they occupy broadly similar microhabitats and depths, making the functional role of GFPs ambiguous, there is some evidence that green morphs may competitively displace brown morphs over extended time periods in very shallow water (Weidenmann *et al*, 2007). Conversely, at least one study has shown that brown morphs were more successful in pairwise contests over space, however this was not investigated in conjunction with a light intensity stressor (Fàbregas-Gumara, 2014). Here, we examine the role of colour morphology and light acclimation on phototaxis in *A. viridis*. Our objectives were to 1) test whether *A. viridis* exhibits positive phototaxis at all; 2) test the hypothesis that phototactic behaviour differs between green and brown morphs of this species (due to differences in preferred light environment); and 3) ask whether phototactic behaviour is modified by prior acclimation to a low light intensity environment.

Methods

Animal collection and husbandry

40 green and brown morphs of *A. viridis* were collected from subtidal locations in the vicinity of Falmouth, Cornwall, UK, and housed in 2 recirculating seawater aquarium systems, consisting of two bath-style tanks each (dimensions 120cmx20cmx60cm, 144L capacity). 10 individuals per morph were acclimated to either a high or low light intensity conditions. Light conditions were created

using overhead, aquarium-grade, LED bars (Aquaray Aquabeam Natural Daylight – Simulating full-spectrum sunlight). Light intensity in the high light acclimation tank was 640 lux in centre radiating to 200 in the corners, and in the low light acclimation tank was 140 lux in the centre radiating to 30 in the corners). Light intensities were ~6 times greater at any given point in the high light tank relative to the equivalent point in the low light tank. Individuals were left for 4 weeks to acclimate to light conditions and were fed 2 days before experimentation. Each acclimation and experimental tank was shrouded to prevent external light. Temperature was controlled via an external cooler set to $15^{\circ}\text{C} \pm 1^{\circ}\text{C}$. Salinity was maintained at 34-35 ppt. Filtered water entered the tanks at one end and exited at the other to create a continuous flow across the tank.

Phototaxis experiments

5 individuals at a time were subjected to a light intensity gradient (that spanned the length of each experimental tank) to avoid overcrowding and minimise potential competition between individuals. Brown and green morphs were tested separately to avoid inter-morph competition that would influence movement in relation to light intensity. The gradient was created by fixing an aquarium LED bar at one end of each experimental tank. Light intensity was calibrated for distance from the LEDs using a Seneye REEF lux meter. Light intensity was measured at the left edge, centre, and right edge across the width of the experimental tanks, and at intervals of 50mm along the length of each tank. Individuals were transferred from the acclimation tanks and positioned in the dark end of each experimental tank, at a common origin 750mm away from the LEDs' position. The maximum distance away from the LED was 950mm to allow negative phototaxis. We measured the distance from the starting location towards the LED light source (using the position of the centre of the oral disk to determine an individuals location) every 24 hours for 6 days. This timeframe was chosen based on the responses seen during the pilot study. An example diagram of the experimental setup is shown in figure A2 in the Appendix.

Directional water flow within tanks (associated with the recirculation system) occurred in the same axis as the light intensity gradient, therefore the experiment was repeated for all individuals with the light gradient reversed to standardise for water movement and/or oxygen concentration (i.e., in trial 1 water flow direction and the light intensity gradient were concurrent, and in trial 2 water flow opposed

the light gradient). Whilst the same individuals were tested with water flow in both directions, their individual IDs could not be established and therefore data subsets were analysed separately. Newly collected individuals would have been used in an ideal scenario; however, COVID 19 disruptions limited available acclimation space and time. The resulting data from each water flow direction was tested separately to maintain independence.

Individuals were weighed at the end of each experiment by gently blotting away excess water until a stable weight was recorded, to identify the effect of mass (i.e., size) on phototactic responses. This is not a justifiable method for identifying individuals and was used only to investigate whether larger individuals had greater phototactic responses.

Statistical analysis

Two Kruskal-Wallis tests were used to compare the light intensity at final position between groups that represented acclimation condition and morph. Two tests were used to ensure independence, as the same individuals (with unknown ID) were subjected to both water flow directions. Post-hoc Dunn's Tests were used to determine which acclimation and morph groups were different. Due to relatively low sample sizes, the Holm adjustment method was used instead of Bonferroni to maximise power (Aickin and Gensler, 1996). Unpaired Wilcoxon rank sum tests were used to test for the (inferred) effect of water flow on the final position (i.e., the likely 'optimal' intensity).

The total distance moved may be defined as the total distance travelled from the start point over 6 days, which includes both positive and negative phototaxis values, but is not a vector measurement and does not indicate the overall direction of movement. The final position was therefore used to determine the total displacement of individuals over six days. This doesn't account for negative movement, instead providing a vector measurement to determine phototaxis in one direction. The difference between total distance moved and total displacement highlights any negative phototaxis during the six-day period, indicating an individual's sensitivity to the light intensity gradient or random, unrelated movement. Distance was found to be a good proxy for predicting light intensity and was therefore used to quantify phototaxis over time. However, the attenuation of light intensity in all directions from the light source is a product of

the inverse-square law and must be considered when comparing distance and light intensity.

We used two linear 'random slope' mixed effect models to determine the effect of acclimation group and morph on the phototaxis responses over the six-day period, one for each water flow direction. In these models, the response variable was distance moved from the starting point towards the light per day, with fixed effects of time, morph, acclimation condition, and the interaction between morph and acclimation condition. A random effect of ID was used to account for non-independence of the 6 repeat observations per individual (i.e., position on day 1 to day 6). This would highlight variation in phototactic responses between acclimation groups and morphs before individuals reached their final positions. The starting position was 0mm for all individuals, therefore the model included no fixed intercept since distance moved started at 0 for all individuals. Our model is as follows:

$$\text{Distance} \sim 0 + \text{Day} + \text{Acclimation.Group:Day} + \text{Morph:Day} + \text{Acclimation.Group:Morph:Day} + (0 + \text{Day} | \text{ID}), \text{REML} = \text{F}$$

Where 'Day' and 'Day | ID' represent random intercepts and slopes respectively. We fitted the models using maximum likelihood in the Lme4 package (Bates *et al*, 2015) and tested the significance of fixed effects using F tests implemented by the LmerTest package (Kuznetsova, Brockhoff, and Christensen, 2017). The data follows a non-linear logistic pattern; however, we were more interested in the group level effects as opposed to the individual level effects. We therefore averaged the response gradients to extract the group level effects and included individual ID as a random effect to simplify the analysis.

Results

Outliers that were a result of detachment from the base of the tank were removed, so that all responses were a direct result of pedal movement. There were also individuals that divided asexually during experiments, however the distance between the clones remained constant for the remaining days and their responses were consequently averaged. It is also important to consider that vertical and lateral movement was not quantified during the experiments, as the majority of observed movement during the pilot study was along the x axis without large deviations in the y or z axes.

Do individuals of *A. viridis* display positive phototaxis?

The mean distance from the LEDs (of all combined groups) was 600.5 mm (se = 24.2 mm), after starting 750 mm from the LEDs. The majority (75%) of phototaxis is positive, and the percentage of positive phototaxis responses does not differ when water flow is opposing positive phototaxis. We can therefore deduce that *A. viridis* does display positive phototaxis in a laboratory setting, and the number of individuals that exhibit positive phototaxis is not dependent on the direction of water flow. There is evidence of negative phototaxis (20%) and evidence of no movement (5%), that requires investigation into the relationship between light intensity and distance, and the individual phototactic responses over time.

The effect of morph and acclimation condition on final positions after 6 days

There was no difference in final position between groups (acclimation condition x morph) when the water flow and the light gradient were concurrent. There was a significant difference ($H(3) = 13.9, p = 0.003$) in the final position between groups when water flow and light gradient were opposed. The post hoc Dunn's test revealed that HL acclimated brown morphs have a lower final position compared with both LL acclimated morphs (RHLB and RLLB ($Z = 3.07, p < 0.02$) and RHLB and RLLG ($Z = 3.29, p < 0.007$)). LL acclimation therefore results in greater final positions when water flow opposes positive phototaxis, regardless of GFP expression (Figure 1).

How are phototactic responses influenced by acclimation condition?

In the second trial with opposing water flow, positive phototaxis was greater than seen in the concurrent trial, and there was a significant effect of acclimation condition on the rate of phototaxis (Table 1). The concurrent trial showed no effect of acclimation group (Table 2). There was no significant effect of morph in either trial.

Conditional repeatability was calculated for both models by dividing the individual variance by total variance (individual + residual), which gives a standardised random effect size. For the opposing trial, 14.3% of variation that was not explained by fixed effects is explained by among-individual variation. For the concurrent trial, 20.3% is explained by among-individual variation. Individual

variation was not a focus of this investigation, however the repeatability values suggest that among-individual variation should be considered in future phototaxis investigations.

Visualising the model predictions allowed us to see and quantitatively compare the effects of acclimation group and morph (Figure 2). Green morphs exhibit similar average responses over time under both acclimation conditions, however the average responses under both acclimation conditions are greater when water flow opposes positive phototaxis. LL acclimated brown morphs exhibit greater average responses than HL acclimated brown morphs with water flowing in either direction. Positive phototaxis responses and resulting optimal light intensities are greater when the light gradient opposes the direction of water flow, which suggests that either water movement or oxygen concentration is influencing the degree of phototaxis.

Discussion/Conclusion

Here we sought to test for phototactic behaviour in the temperate sea anemone *A. viridis* and whether these responses differ as a result of GFP expression or morph. We found support for our first hypothesis that *A. viridis* does indeed show phototaxis, as seen in other photosymbiotic anemone species. Whilst the majority of movement was positive, some individuals exhibited negative phototaxis at low light intensity which has not been discussed in literature to date. Our second hypothesis that morphs will differ in their final position, inferring an 'optimal' light intensity preference, was not supported by our results and was therefore rejected. The differences between morphs when water flow opposed positive phototaxis were more likely to be an interactive result of acclimation condition. Our third hypothesis that acclimation condition modifies phototaxis is accepted. LL acclimated individuals showed greater phototactic responses than HL acclimated individuals for both morphs. The efficiency of symbionts is therefore the likely driver of phototaxis in *A. viridis* as there is no difference between morphs.

Phototaxis will benefit temperate cnidarians as they can fully exploit variable lighting conditions in coastal environments. It is likely that the combination of autotrophic and heterotrophic energy provision within photosymbioses contribute to the trophic dominance of sea anemones as small benthic predators, particularly within the intertidal zone. Coupled with the high mobility of *A. viridis*,

behaviours such as phototaxis has aided the species' widespread distribution, and provides an adaptability that makes the species so successful.

We found that GFPs did not influence phototaxis as there were no differences in final position or responses over time between morphs. The light intensities used in this investigation were not extreme values and may not have utilised the full photoprotective abilities of GFPs. During the summer, individuals within rockpools will be exposed to a high UV index and GFPs may have a greater influence on phototaxis responses than seen in our investigation. Green morphs may be dominant in very shallow water (Weidenmann *et al*, 2007) as a result of GFP expression, however, this was not reflected by differences in final position between RHLG and RHLB ($p = 0.215$). GFPs must therefore have an alternative function in *A. viridis* that is not photo-enhancing. This species feeds on herbivorous crustaceans and amphipods, and GFPs may serve as an active prey attractant for green morphs, whilst brown morphs may utilise a passive hunting strategy. In addition, it is also possible that GFP expression is simply a vestigial trait in this temperate anemone species.

Phototaxis responses were unexpectedly small and often negative in HL acclimated individuals. When HL acclimated, symbiotic hosts exhibit downregulation on dividing symbionts to curb excessive symbiont density (Xiang *et al*, 2020), with symbiont densities often peaking when individuals are acclimated to an intermediate light intensity, and then reducing when acclimated to dark conditions (Saunders and Muller-Parker, 1997; Lowe *et al*, 2016). Low symbiont densities have reduced photosynthate outputs, and consequently reduce host-symbiont signals. Whilst this may explain the small phototactic responses of HL acclimated individuals, it does not explain the difference in responses of LL acclimated individuals under concurrent water flow than opposing flow.

It is possible that oxygen concentration or water flow limited the movement of individuals, as anemones have been shown to cease phototaxis when oxygen concentrations are high (Fredericks, 1976). In the concurrent trial, the start position for all individuals was close to the experimental tanks' water inputs, where oxygenated water enters the tanks from the filtration systems. Moving water may reduce the thickness of boundary layers surrounding the anemones' surfaces, enabling greater gas exchange and therefore increasing the

concentration of oxygen available for absorption into tissues (Patterson and Sebens, 1989; Patterson, Sebens and Olsen, 1991; Sebens *et al*, 2003). The presence of moving and/or oxygenated water may simulate the oxygen output of symbionts at high light intensity on one side of the host's body, and artificially attract the anemone. Since we observed small but positive phototaxis responses in the concurrent trial, stimulation by photosynthetically derived oxygen concentrations may have outweighed the potentially artificial stimulation by oxygenated water. There may be an equilibrium between phototaxis and oxytaxis (movement in response to oxygen concentration) when light intensity gradients interact with oxygen concentration gradients.

The idea that oxygen concentration influences phototaxis may also explain why responses were larger in the opposing water flow trial. In this case, the light intensity gradient aligned with the oxygen concentration gradient. Greater symbiont densities in LL acclimated individuals increase host and symbiont oxygen demand in the dark, potentially causing oxytaxis in the first few hours/days of the experiment when individuals are in the dark end of the light intensity gradient. Higher light intensity may then kickstart photosynthesis at a critical light intensity and shift the movement driver from oxytaxis to phototaxis.

We were interested in group level effects and did not investigate individual responses in detail. However, basic non-linear modelling of the concurrent trial data follows a general logistic pattern, with a time lag at the start of the experiment and a saturating curve by the end (Figure A3 in Appendix). If oxytaxis is indeed occurring, it may represent the initial acceleration of the logistic curves and have ecological importance in shaded temperate environments. Our repeatability calculations suggest that individual variation is an important consideration for further study into these relationships.

Our results explain the similar depth distributions of both morphs in the wild. The final position from the LEDs was recorded at 6 days, which was sufficient for the anemones to settle in their preferred locations within the tank as lighting conditions remained constant (including a 12h diurnal cycle to reduce stress). In the wild, lighting conditions will never remain constant and continuous phototaxis will result in short-term energy demand by the host that must be supplemented by photosynthates (Taylor 1969; Bachar *et al*, 2007). Phototaxis is particularly important for individuals residing at depth where preferable light intensity

microhabitats are sparse and short-term energy demand is high, exemplified by the LL acclimated individuals in our investigation.

In conclusion, the phototactic responses of *A. viridis* are complex and highly variable, with acclimation to low light intensity (a proxy for higher symbiont density) and direction of water flow being the most important drivers of movement. The functional role of GFPs in the *A. viridis* example does not influence the phototactic response and remains elusive. Future study should investigate *A. viridis* oxytaxis, the potential transition from oxytaxis to phototaxis at certain light intensities, and how this 'photoxytaxis' influences the distribution of individuals in the field. It would be useful to correlate these responses with predicted light conditions for future temperate environments and investigate whether GFPs become more beneficial traits as opposed to vestigial traits as temperate environments become sub-tropical. An alternative direction could also be taken, looking at the hunting methods of morphs. For example, do GFPs in green morphs act as prey attractants in this species (as they do in sea jellies), whilst brown morphs have a sit-and-wait strategy and prey on timid species in the shadows? Understanding the species-specific mechanisms that underpin symbiosis, particularly the interaction between host adaptation, symbiont efficiency, and the local microhabitat, is essential to determine the impacts of changing environments. Only then will scientists be able to make accurate predictions of cnidarian species distribution, richness, and the knock-on impacts of climate change on trophic interactions within important systems such as coral reefs.

Figures and Tables

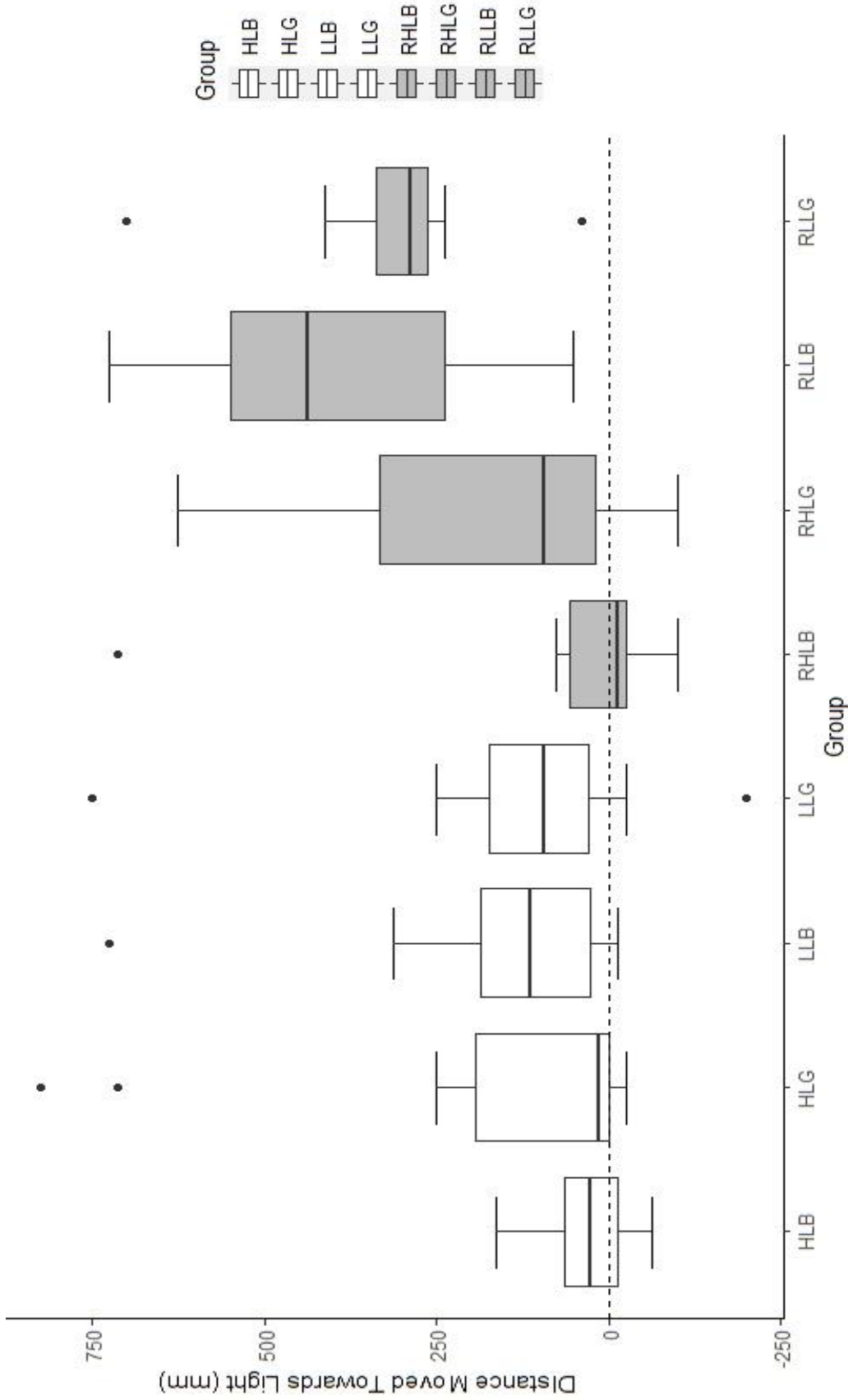


Figure 1: Distance moved towards the LED light source after 6 days for all groups when water flow is in the direction of positive movement (white bars) or in the direction of negative movement (grey bars). Groups relate to the acclimation condition (high light or low light) and morph (green or brown). The R in groups with grey shading refers to the direction of water flow being reversed. The number of individuals in each group ranges from 8 to 11 as a result of death or splitting (asexual reproduction) mid experiment. Black points outside the interquartile ranges are individual outliers, however at time of measurement the individuals were attached to the surface so movement was achieved either by pedal disk motion or movement by the water current following detachment.

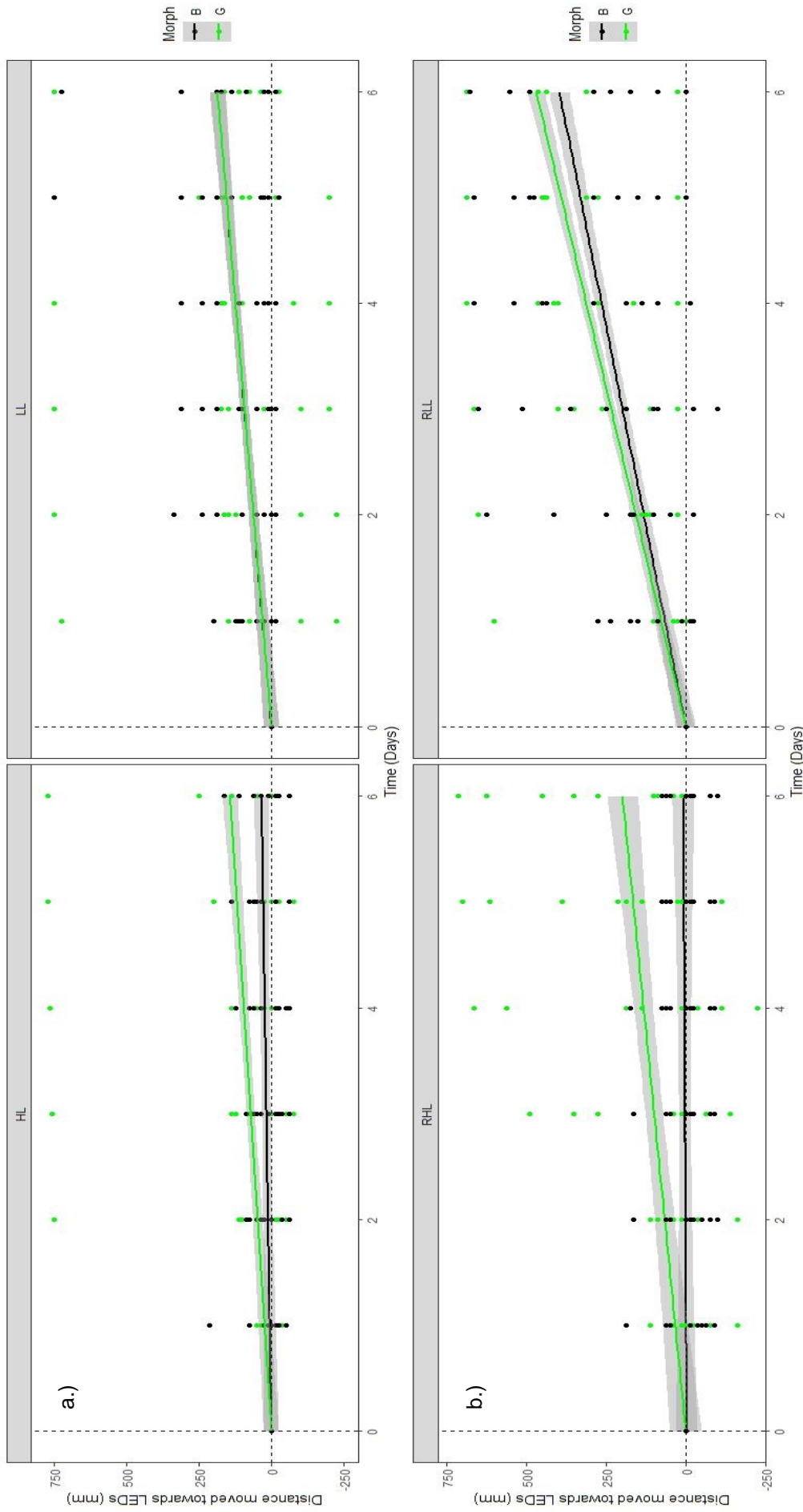


Figure 2: The displacement of green morphs (green) and brown morphs (black) from the starting point towards the light source over the 6-day period. Points show the raw positions of individuals that follow a non-linear pattern, with a regression line representing the mixed effect model used to observe differences between groups. a.) The responses of HL (left) and LL (right) acclimated individuals when positive phototaxis and water flow were concurrent. b.) The same individual responses when positive phototaxis and water flow were opposing. HL acclimated green individuals exhibit greater phototaxis responses than HL acclimated brown individuals regardless of water flow direction. Brown morphs exhibit greater phototaxis responses when acclimated to LL than HL, and their LL responses match that of LL green morphs. Reversing the direction of water flow increases the phototactic response of both green and brown morphs that have been LL acclimated.

Table 1: The lmer output for the opposing water flow trial. Estimate values indicate the fixed effect size and direction, supported by an F test for significance.

Fixed Effects	Estimate	Std. Error	F value	p value
Day	66.0	13.0	25.6	<0.005
Day:Acclimation.GroupHL	-61.9	18.0	17.5	<0.005
Day:MorphG	28.9	17.1	2.56	0.118
Day:Acclimation.GroupLL:MorphG	-16.9	25.6	0.437	0.513
Random Effects	Variance	Std. Dev		
ID	1435	37.9		
Residual	8613	92.8		

Table 2: The lmer output for the concurrent water flow trial. Estimate values indicate the fixed effect size and direction, supported by an F test for significance.

Fixed Effects	Estimate	Std. Error	F value	p value
Day	30.9	13.2	5.50	0.0241
Day:Acclimation.GroupHL	-25.4	18.7	1.31	0.259
Day:MorphG	18.0	18.7	0.348	0.559
Day:Acclimation.GroupLL:MorphG	-20.5	26.4	0.602	0.442
Random Effects	Variance	Std. Dev		
ID	1667	40.8		
Residual	6561	81.0		

General Discussion/Conclusion

Understanding the physiological and behavioural response of cnidarian-algae symbioses to varying abiotic stressors will be an invaluable resource for predicting climate change impacts on shallow coastal environments. Cnidarian polymorphs and their response to variations in light intensity has not been studied in enough detail to fully comprehend the primary functions of photoadaptations (such as GFPs) that may vary within and between species. We investigated a model cnidarian-algae symbiosis to determine whether colour morphs differ in their physiological and behavioural responses to varied light intensity, to better understand the functional role of GFPs in temperate environments.

In chapter 1 we developed an OS photo-respirometer to make the measurement of photosynthesis irradiance responses more tractable. Our photo-respirometer produced clear and consistent PI curves that were used to identify clear photosynthetic responses to increasing light intensity – a research topic that presents multiple challenges in apparatus design. Photo-respirometry apparatus must be designed to overcome constraints associated with organismal size and husbandry requirements, whilst maintaining a constant temperature and limiting sources of signal drift (such as background microbial respiration). Our design overcame these challenges whilst also presenting an opportunity for modification, allowing researchers to investigate the effects of temperature, pH, and other environmental parameters. For example, the temperature controlled subject chamber enables investigation into the effect of varied temperatures on photo-symbiosis in *A. viridis*, or the chamber could be interchanged entirely with a continuous flow setup for measuring oxygen consumption during stress events in fish. In addition, the system does not involve materials that corrode and is easy to clean, making it ideal for both marine and freshwater applications. OS technology will likely become an important component in biological research and teaching applications, as equipment can be easily modified at low expense. Observing the responses of various key organisms such as corals to multiple environmental stressors has helped to shape marine management decisions that mitigate the effects of climate change.

Physiological adaptation often drives behaviour, with adaptations to environmental conditions such as light intensity enabling organisms to interact

with specific microhabitats. Whilst we know this to be the case for many motile organisms, it does not appear to be true for the *A. viridis* example. In chapter 1 we investigated the photosynthetic responses of GFP expressive and non-expressive morphs within *A. viridis*. Contrary to the theory that GFPs enhance photosynthesis at high light intensity, there was no apparent advantage of green morphs over brown morphs in our investigation. This suggests that GFPs may not have the photo-enhancing function that we initially hypothesised, and their expression in this species may have alternative functions. Firstly, primary GFP functions are varied, with tropical coral species using them to reduce UV-induced cellular damage whilst sea jellies (such as hydromedusae) use GFPs to attract prey (Haddock and Dunn, 2015). This increases difficulty in predicting their primary function for different cnidarian species. Temperate species such as *A. viridis* will not experience the degree of UV radiation as the tropics and does not feed on the same prey as other cnidarians like sea jellies, therefore the primary role of their GFPs remains unknown. Secondly, the distribution of *A. viridis* includes northern Mediterranean coasts. It is possible that GFPs were once a useful adaptation to high light stress for individuals that inhabit warmer climates, and that the expression of GFPs in temperate environments are potentially becoming a vestigial trait. We were interested to see how the results of our physiological investigation translated into behaviour and whether morphs would differ in behavioural responses to light intensity.

In chapter 2 we found that phototactic responses were exhibited by *A. viridis* and that acclimation to low light intensity produced greater average phototactic responses. Crucially, we found no significant differences in phototaxis between morphs, which again suggests that temperate GFPs or colour morphology may not influence adaptation and acclimation to light intensity. The most interesting conclusion however is that phototaxis may be influenced by the direction of water flow. When water flow was concurrent with the light intensity gradient, phototactic responses were smaller than when water flow and light intensity were countercurrent. This suggests that either the movement of water, or the oxygen concentration within the water, or a combination of the two, influenced phototaxis. There may be a potential link between oxygen concentration and phototaxis (Fredericks, 1976), though this interaction is not well investigated. We suggest that phototaxis may not be a direct response to light intensity, but is mediated by

oxygen concentration, which is indirectly correlated with light intensity as a result of oxygen production during photosynthesis. In this case, oxygen gradients within the water column may artificially attract hosts and result in an equilibrium between phototaxis and oxytaxis. This 'photoxytaxis' is potentially driven by oxygen gradients within the host, generated by differences in rates of symbiont photosynthesis on 'shaded' or 'exposed' sides of the host animal. Greater oxygenation is often caused by turbulent water, which itself may be attractive to the host anemone as a source of greater heterotrophic food availability. Whilst there may be a possibility of thigmotaxis (response to the mechanical aspect of turbulent water), *A. viridis* does not show tentacle retraction in response to mechanical stimuli (Weinbauer, Nussbaumer, and Patzner, 1981). Therefore, it is more likely that *A. viridis* is exhibiting oxytaxis rather than thigmotaxis in response to water flow. The resulting 'photoxytaxis' behaviour may be a mechanism for optimising autotrophic or heterotrophic energy intake in changing environments. This would be an important adaptation at the intertidal zone, where rockpools channel water movement and concentrate small free-swimming arthropods or dead crustaceans that forms the majority of *A. viridis*'s diet.

The results and conclusions presented in chapters 1 and 2 further our understanding of how the *A. viridis* – *Symbiodinium* symbiosis, suggesting that colour morphology is unlikely an adaptation associated with light. The results suggest that GFPs are not necessarily beneficial for photosynthesis within temperate photosymbioses, as there were no clear differences between morphs in either the physiological or behavioural experiments. Future studies on GFP function should therefore aim to determine whether GFPs are vestigial traits in temperate photosymbioses or whether their primary role involves prey or symbiont attraction in cnidarians such as *A. viridis*.

The effect of water flow should also be investigated further, determining whether 'photoxytaxis' drives the movement of photosymbiotic cnidarians within their environment, or whether individuals position themselves to maximise food capture. This is an important development as it would alter the current perception of temperate photosymbiotic behaviour. Other temperate anemones such as *Anthopleura elegantissima* respond to oxygen concentration as opposed to light intensity (Fredericks, 1976). It is possible that temperate cnidarians can detect differences in symbiont photosynthesis across their body and may use this

stimulus to undertake phototaxis as opposed to direct light sensing. Whilst Fredericks theorised that *A. elegantissima* does not respond to light intensity, this was not the case for *A. viridis*. 'Photoxytaxis' is therefore a more appropriate term to describe this particular behaviour in temperate sea anemones and may also be applicable for other marine photosymbioses.

Appendices

Chapter 1:

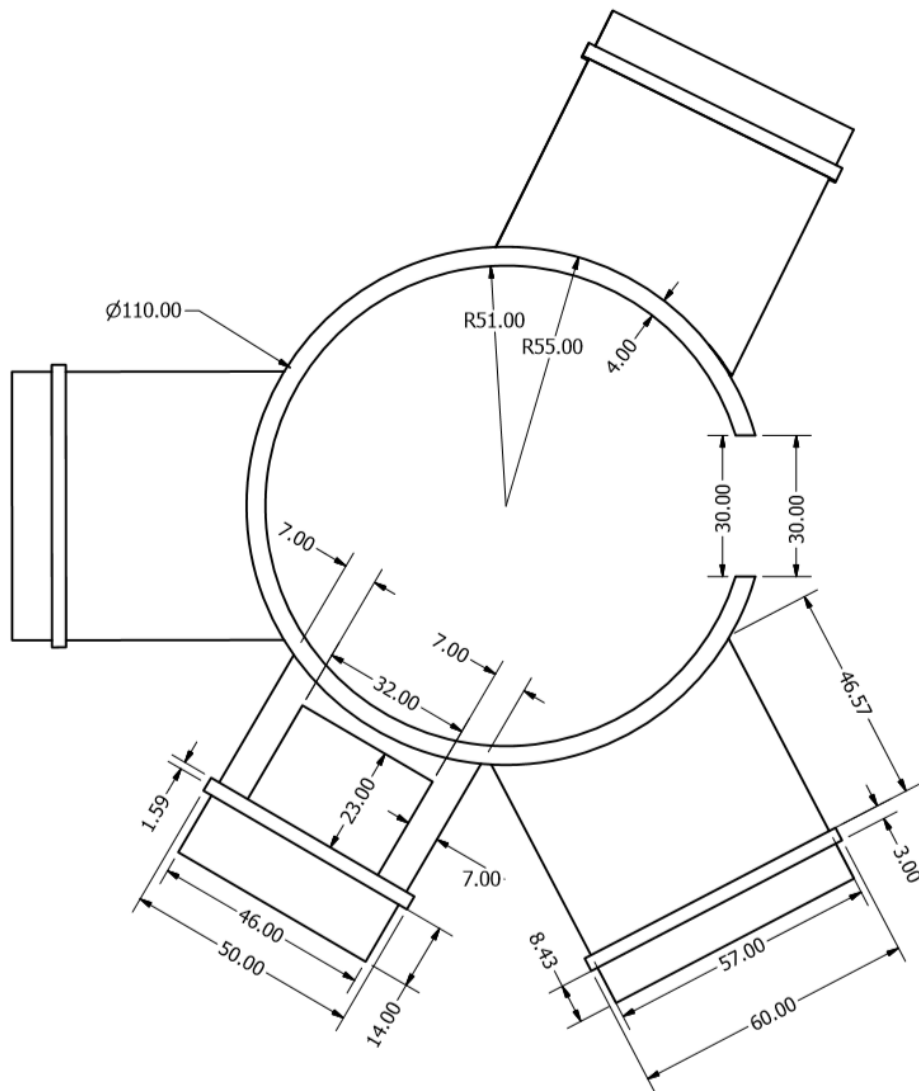


Figure A1: Technical drawing of the lighting rig housing with dimensions in mm. The depth and inner diameter of the housing is dependent on the size of the subject chamber being used and tolerances should be small enough to prevent light from entering the chamber when LEDs are off (~1mm).

RPi wiring diagram:

https://www.raspberrypi.org/documentation/hardware/raspberrypi/schematics/rpi_SCH_3b_1p2_reduced.pdf

PicoBuck driver technical sheet:

http://www.farnell.com/datasheets/2100145.pdf?_ga=2.236790977.1728830886.1559755882-887172721.1559755882&_gac=1.61621854.1559755882.CjwKCAjw0N3nBRBvEiwAHMwvNoCjTVR9re91PCMpj84tL2X-EPj3duDBSvRp9XNwblh6mMQrCfh0qxoCBC8QAvD_BwE

Table A1: Pin layout of the RPi with corresponding function and which input and output pins have been utilised by our system. The high number of pins shows how versatile the RPi is as an OS system, and the potential for complex systems to be created.

Function	Pin	Pin	Function	Current Use
3.3v	1	2	5v	
GPIO2	3	4	5v	relay power
GPIO3	5	6	GND	relay ground
GPIO4	7	8	GPIO14	
GND	9	10	GPIO15	to relay – cooling fans
GPIO17	11	12	GPIO18	to relay – circulation pump
GPIO27	13	14	GND	
GPIO22	15	16	GPIO23	to relay – recirculation pump
3.3v	17	18	GPIO24	
GPIO10	19	20	GND	
GPIO9	21	22	GPIO25	
GPIO11	23	24	GPIO8	
GND	25	26	GPIO7	
DNC	27	28	DNC	
GPIO5	29	30	GND	
GPIO6	31	32	GPIO12	
GPIO13	33	34	GND	LED driver ground
GPIO19	35	36	GPIO16	to LED driver LED1 in
GPIO26	37	38	GPIO20	to LED driver LED2 in
GND	39	40	GPIO21	to LED driver LED3 in

Chapter 2:

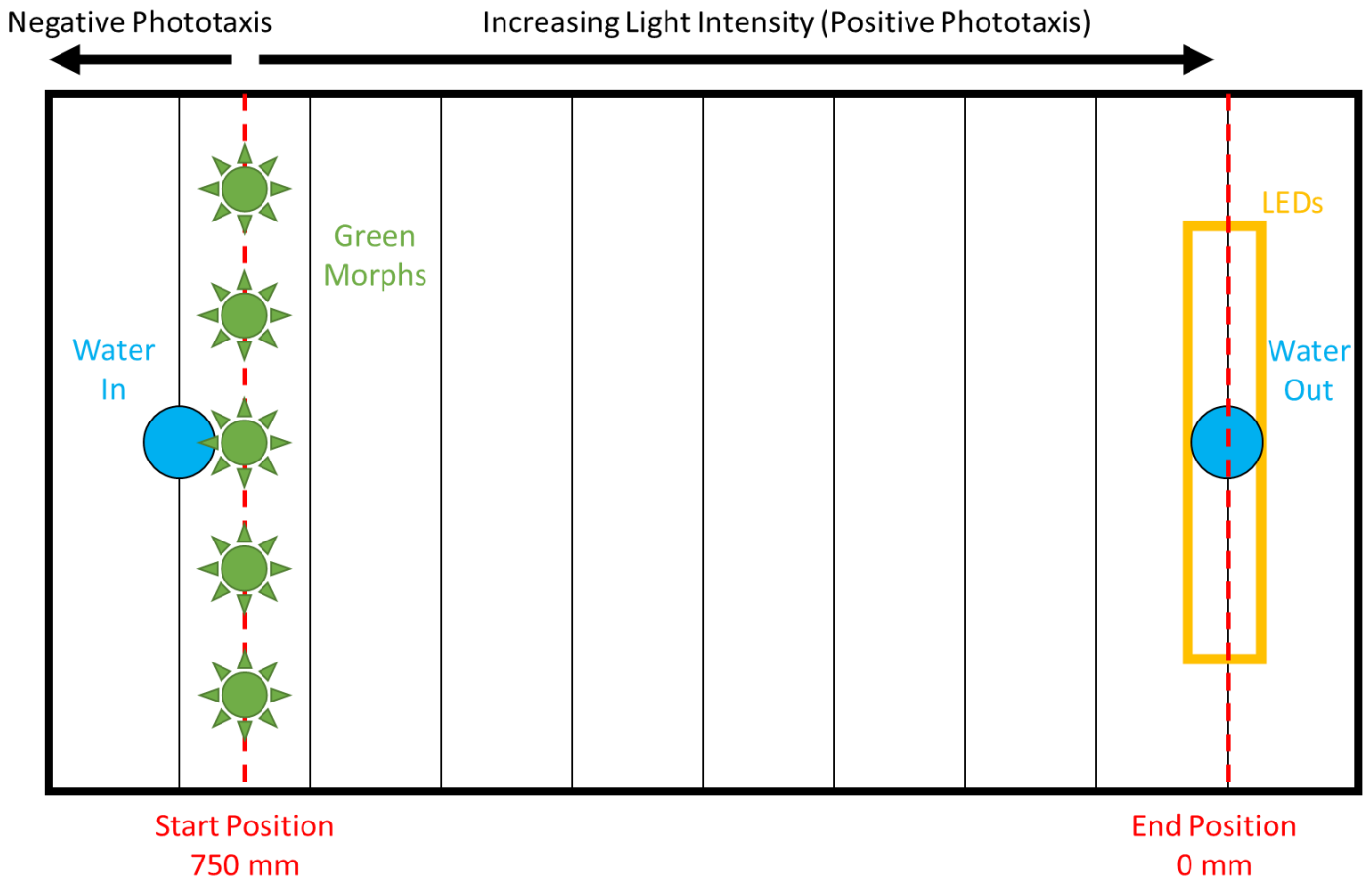


Figure A2: Experimental setup for phototaxis trials. 5 individuals (in this case green morphs at day 1) were positioned 750 mm from the midpoint of the LED light source (0 mm). Light intensity increased as distance towards the LEDs decreased. Blue circles represent the water input (left) and output (right) pipes that created a steady continuous water flow from left to right. The vertical grid was used to calculate the position of individuals per day.

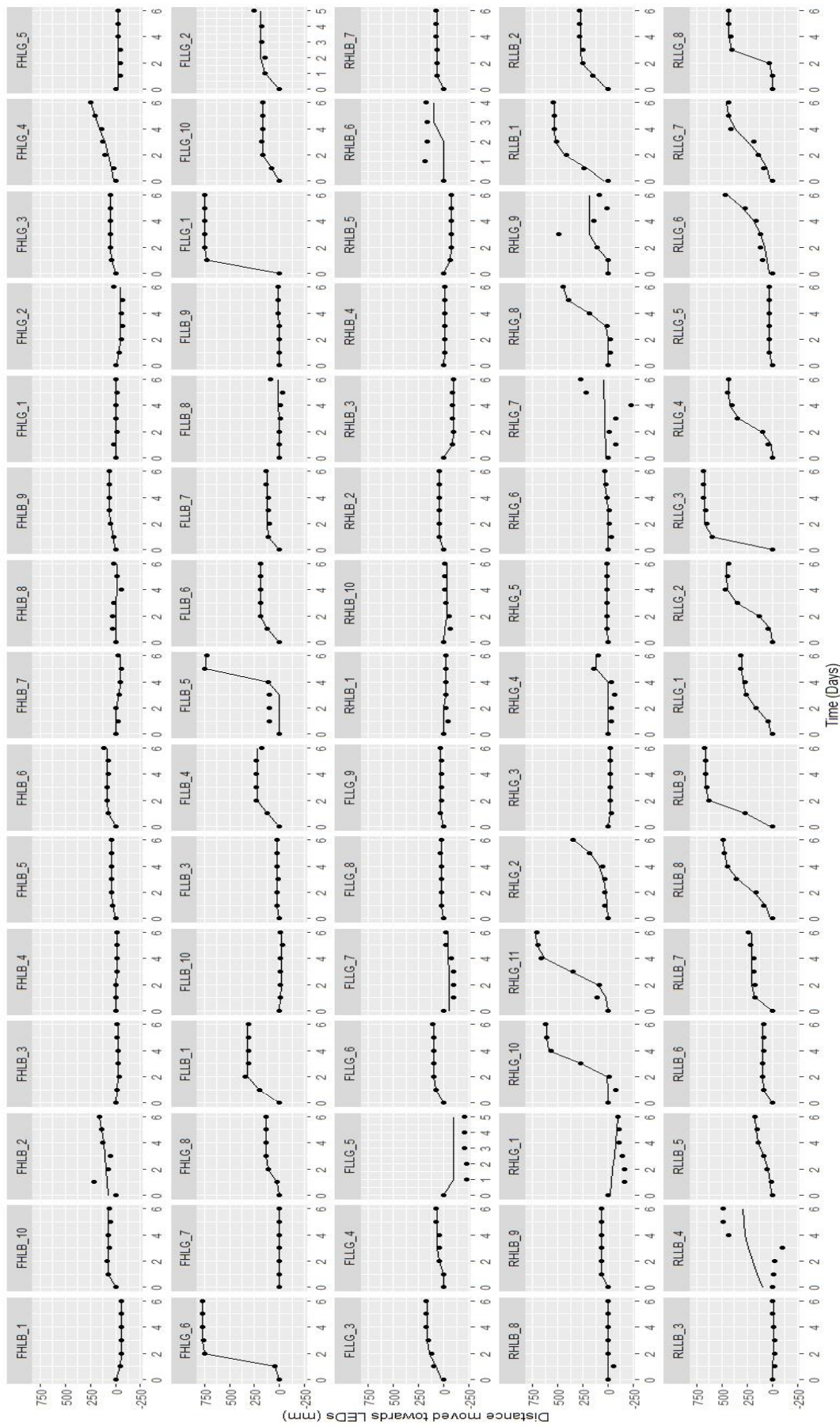


Figure A3: The individual phototaxis responses over a period of 6 days, overlaid with fitted values (i.e., model predictions). A nonlinear logistic model was used to explain the pattern of movement, fitted using lmer in Rstudio. This figure shows the potential for individual preference to be an important factor when investigating phototaxis responses. Investigating these preferences were beyond the scope of this investigation but are a sound foundation for future studies.

Bibliography

Aickin, M. and Gensler, H. (1996) Adjusting for multiple testing when reporting research results: the Bonferroni vs Holm methods, *American Journal of Public Health*, 86(5): 726-728.

Aihara, Y., Maruyama, S., Baird, A.H., Iguchi, A., Takahashi, S. and Minagawa, J. (2019) Green Fluorescence from Cnidarian Hosts Attracts Symbiotic Algae, *PNAS*, 116(6): 2118-2123.

Andersson, A. J., Kline, D. I., Edmunds, P. J., Archer, S. D., Bednaršek, N., Carpenter, R. C., Chadsey, M., Goldstein, P., Grottoli, A. G., Hurst, T. P., King, A. L., Kübler, J. E., Kuffner, I. B., Mackey, K. R. M., Menge, B. A., Paytan, A., Riebesell, U., Schnetzer, A., Warner, M. E. and Zimmerman, R. C. (2015) Understanding ocean acidification impacts on organismal to ecological scales, *Oceanography*, 28(2): 16-27.

Bachar, A., Achituv, Y., Pasternak, Z. and Dubinsky, Z. (2007) Autotrophy versus heterotrophy: The origin of carbon determines its fate in a symbiotic sea anemone, *Journal of Experimental Marine Biology and Ecology*, 349(2): 295-298.

Bates, D., Mächler, M., Bolker, B. and Walker, S. (2015) Fitting linear mixed-effects models using lme4, *Journal of Statistical Software*, 67(1): 1-48.

Begood, A. A., Bracken, M. E. S., Ryan, W. H., Levell, S. T. and Wulff, J. (2020) Nutritional drivers of adult locomotion and asexual reproduction in a symbiont-hosting sea anemone *Exaiptasia diaphana*, *Marine Biology*, 167, (article) 39. <https://doi.org/10.1007/s00227-020-3649-3>.

Bellwood, D. R., Hoey, A. S. and Hughes, T. P. (2011) Human activity selectively impacts the ecosystem roles of parrotfishes on coral reefs, *Proceedings of the Royal Society B*, 279: 1621-1629.

Brown, B.E. (1997) Coral bleaching: causes and consequences, *Coral Reefs*, 16: 129-138.

Byrnes, E. E., Lear, K. O., Morgan, D. L. and Gleiss, A. C. (2020) Respirometer in a box: development and use of a portable field respirometer for estimating oxygen consumption of large-bodied fishes, *Journal of Fish Biology*, 96(4): 1045-1050.

Chang, W., Cheng, J., Allaire, J.J., Xie, Y. and McPherson, J. (2020). shiny: Web Application Framework for R. R package version_1.4.0.2. <https://CRAN.R-project.org/package=shiny>.

Chown, S. L., Hoffmann, A. A., Kristensen, T. N., Angilletta Jr, M. J., Stenseth, N. C. and Pertoldi, C. (2010) Adapting to climate change: a perspective from evolutionary physiology, *Climate Research*, 43: 3-15.

Cohen, I. and Dubinsky, Z. (2015) Long term photoacclimation responses of the coral *Stylophora pistillata* to reciprocal deep to shallow transplantation: photosynthesis and calcification, *Frontiers in Marine Science*, 2: 45.

Cowen, R. (1988) The role of algal symbiosis in reefs through time, *PALAIOS*, 3(2): 221-227.

Cumbo, V. R., van Oppen, M. J. H. and Baird, A. H. (2018) Temperature and *Symbiodinium* physiology affect the establishment and development of symbiosis in corals, *Marine Ecology Progress Series*, 587: 117-127.

Cunning, R. and Baker, A.C. (2012) Excess algal symbionts increase the susceptibility of reef corals to bleaching, *Nature Climate Change*, 3: 259-262.

Davy, S. K., Allemand, D. and Weis, V. M. (2012) Cell biology of cnidarian-dinoflagellate symbiosis, *Microbiology and Molecular Biology Reviews*, 76(2): 299-261.

Dean, A.D., Minter, E.J.A., Sørensen, M.E.S., Lowe, C.D., Cameron, D.D., Brockhurst, M.A. and Jamie Wood, A. (2016) Host control and nutrient trading in a photosynthetic symbiosis, *Journal of Theoretical Biology*, 405: 82-93.

Decelle, J. (2013) New perspectives on the functioning and evolution of photosymbiosis in plankton, *Communicative & Integrative Biology*, 6:4.

Deek, F.P. and McHugh, J.A.M. (2008) OS: Technology and Policy, New York, Cambridge University Press, Available at: https://books.google.co.uk/books?hl=en&lr=&id=PA-Rhb_QSAwC&oi=fnd&pg=PR1&ots=IVtU1y1VC8&sig=0WjvLuqeWRFwzS8BykmiqyblpWs&redir_esc=y#v=onepage&q&f=false [Accessed 13 May 2020].

- Dove, S.G., Hoegh-Guildberg, O. and Ranganathan, S. (2001) Major colour patterns of reef-building corals are due to a family of GFP-like proteins, *Coral Reefs*, 19: 197-204.
- Drown, M. K., DeLiberto, A. N., Crawford, D. L. and Oleksiak, M. F. (2020) An innovative setup for high-throughput respirometry of small aquatic animals, *bioRxiv*. <https://doi.org/10.1101/2020.01.20.912469>.
- Dubinsky, Z. and Jokiel, P.L. (1994) Ratio of energy and nutrient fluxes regulates symbiosis between zooxanthellae and corals, *Pacific Science*, 48(3): 313-324.
- Eiler, P. H. and Peeters, J. C. (1988) A model for the relationship between light intensity and the rate of photosynthesis in phytoplankton, *Ecological Modelling*, 42: 199-215.
- Eyal, G., Weidenmann, J., Grinblat, M., D'Angelo, C., Kramarsky-Winter, E., Treibitz, T., Ben-Zvi, O., Shaked, Y., Smith, T. B., Harii, S., Denis, V., Noyes, T., Tamir, R. and Loya, Y. (2015) Spectral diversity and regulation of coral fluorescence in a mesophotic reef habitat in the Red Sea, *PLoS ONE* 10(6): e0128697. <https://doi.org/10.1371/journal.pone.0128697>.
- Fàbregas-Gumara, T. (2014) Comportamiento agresivo intraespecífico e interespecífico de *Anemonia viridis* en el intermareal, *Anales Universitarios de Etología*, 8: 67-75.
- Fisher, D. K. and Gould, P. J. (2012) Open-source hardware is a low-cost alternative for scientific instrumentation and research, *Modern Instrumentation*, 1: 8-20.
- Foo, S.A., Liddell, L., Grossman, A. and Caldeira, K. (2020), Photo-movement in the sea anemone *Aiptasia* influenced by light quality and symbiotic association, *Coral reefs*, 39(1): 47-54.
- Fransolet, D., Roberty, S. and Plumier, J-C. (2012) Establishment of Endosymbiosis: The Case of Cnidarians and *Symbiodinium*, *Journal of Experimental Marine Biology and Ecology*, 420-421: 1-7.
- Fredericks, C.A. (1976), Oxygen as a limiting factor in phototaxis and in intracolonial spacing of the sea anemone *Anthopleura elegantissima*, *Marine Biology*, 38: 25-28.

Furla, P., Richier, S. and Allemand, D. (2011) Physiological Adaptation to Symbiosis in Cnidarians, *Coral Reefs: An Ecosystem in Transition*, Dordrecht, Springer, Available at: <https://link.springer.com/chapter/10.1007/978-94-007-0114-4_12#citeas> [Accessed 13 May 2020].

Griffiths, A. G. F., Kemp, K. M., Garrett, J. K. and Griffiths, D. J. (2017) Sonic Kayaks: Environmental monitoring and experimental music by citizens, *PLoS Biology*, 15(11).

Haddock, S. H. D. and Dunn, C. W. (2015) Fluorescent proteins function as a prey attractant: experimental evidence from the hydromedusa *Olindias formosus* and other marine organisms. *Biology Open*, 4(9): 1094-1104.

Hansel, C. M. and Diaz, J. M. (2021) Production of extracellular reactive oxygen species by marine biota, *Annual Review of Marine Science*, 13(1): 177-200.

Harley, C. D. G., Randall Hughes, A., Hultgren, K. M., Miner, B. G., Sorte, C. J. B., Thornber, C. S., Rodriguez, L. F., Tomanek, L. and Williams, S. L. (2006) The impacts of climate change in coastal marine systems, *Ecology Letters*, 9: 228-241.

Hoegh-Guldberg, O., Poloczanska, E. S., Skirving, W. and Dove, S. (2017) Coral reef ecosystems under climate change and ocean acidification, *Frontiers in Marine Science*, 4: 158.

Hope, J. (2008) *Biobazaar: The OS Revolution and Biotechnology*, Harvard University Press.

Huston, M. A. (1985) Patterns of species diversity on coral reefs, *Annual Review of Ecology and Systematics*, 16(1): 149-177.

Johannes, R.E., Wiebe, W.J., Crossland, C.J., Rimmer, D.W. and Smith, S.V. (1983) Latitudinal limits of coral reef growth, *Marine Ecology Progress Series*, 11: 105-111.

Johnson, K. M. and Hofmann, G. E. (2020) Combined stress of ocean acidification and warming influence survival and drives differential gene expression patterns in the Antarctic pteropod, *Limacina helicina antarctica*, *Conservation Physiology*, 8: coaa013. doi:10.1093/conphys/coaa013.

Kahng, S.E., Hochberg, E.J., Apprill, A., Wagner, D., Luck, D.G., Perez, D. and Bidigare, R.R. (2012) Efficient light harvesting in deep-water zooxanthellate corals, *Marine Ecology Progress Series*, 455: 65-77.

Kuznetsova, A., Brockhoff, P. B. and Christensen, R. H. B. (2017) LmerTest package: Tests in linear mixed effects models, *Journal of Statistical Software*, 82(13): 1-26.

Lehnert, E.M., Burriesci, M.S. and Pringle, J.R. (2012) Developing the anemone *Aiptasia* as a tractable model for Cnidarian-dinoflagellate symbiosis: The transcriptome of aposymbiotic *A. pallida*, *BMC Genomics*, 13: 271.

Lowe, C.D., Minter, E.J., Cameron, D.D. and Brockhurst, M.A. (2016) Shining a light on exploitative host control in a photosynthetic endosymbiosis, *Current Biology*, 26: 207-211.

Mallien, C., Porro, B., Zamoum, T., Olivier, C., Wiedenmann, J., Furla, P. and Forcioli, D. (2017) Conspicuous morphological differentiation without speciation in *Anemonia viridis* (Cnidaria, Actiniaria), *Systematics and Biodiversity*, 16(3): 271-286.

Mantha, S.V., Johnson, G.A. and Day, T.A. (2001) Evidence from action and fluorescence spectra that UV-induced violet-blue-green fluorescence enhances leaf photosynthesis, *Photochemistry and Photobiology*, 73(3): 249-256.

Monaco, C. J. and Helmuth, B. (2011) Tipping points, thresholds and the keystone role of physiology in marine climate change research, *Advances in Marine Biology*, 60: 123-160.

Muller-Parker, G. and Davy, S. K. (2001) Temperate and tropical algal-sea anemone symbioses, *Invertebrate Biology*, 120(2): 104-123.

Muller-Parker, G., D'elia, C.F. and Cook, C.B. (2015) Interactions between corals and their symbiotic algae, in Birkeland, C. ed, (2015) *Coral Reefs in the Anthropocene*, Dordrecht, Springer: 99-116.

Mundy, C.N. and Babcock, R.C. (1998) Role of light intensity and spectral quality in coral settlement: Implications for depth-dependent settlement? *Journal of Experimental Marine Biology and Ecology*, 223(2): 235-255.

- Myriokefalitakis, S., Daskalakis, N., Mihalopoulos, N., Baker, A. R., Nenes, A. and Kanakidou, M. (2015) Changes in dissolved iron deposition to the oceans driven by human activity: a 3-D global modelling study, *Biogeosciences*, 12: 3973-3992.
- Patterson, M. R. and Sebens, K. P. (1989) Forced convection modulates gas exchange in cnidarians, *PNAS*, 86: 8833-8836.
- Patterson, M. R., Sebens, K. P. and Olsen, R. R. (1991) In situ measurements of flow effects on primary production and dark respiration in reef corals, *Limnology and Oceanography*, 36(5): 936-948.
- Pearce, J.M. (2012) Building Research Equipment with Free, OS Hardware, *Science*, 337(6100): 1303-1304.
- Pearce, V.B. (1974) Modification of sea anemone behaviour by symbiotic zooxanthellae: Phototaxis, *The Biological Bulletin*, 147(3): 630-640.
- Petrou, K., Ralph, P. J. and Nielsen, D. A. (2017) A novel mechanism for host-mediated photoprotection in endosymbiotic foraminifera, *The ISME Journal*, 11: 453-462.
- Philippart, C.J.M., Cadée, G.C., Raaphorst, W.V. and Riegman, R. (2000) Long-term phytoplankton-nutrient interactions in a shallow coastal sea: Algal community structure, nutrient budgets, and denitrification potential, *Limnology and Oceanography*, 45(1): 131-144.
- Picciani, N., Kerlin, J. R., Sierra, N., Swafford, A. J. M., Ramirez, M. D., Roberts, N. G., Cannon, J. T., Daly, M. and Oakley, T. H. (2018) Prolific origination of eyes in cnidaria with co-option of non-visual opsins, *Current Biology*, 28(15): 2413-2419.
- Porro, B., Mallien, C., Hume, B. C. C., Pey, A., Aubin, E., Christen, R., Voolstra, C. R., Furla, P. and Forcioli, D. (2020) The many faced symbiotic Snakelocks anemone (*Anemonia viridis*, Anthozoa): host and symbiont genetic differentiation among colour morphs, *Heredity*, 124: 351-366.
- Quick, C., D'Angelo, C. and Wiedenmann, J. (2018) Trade-offs associated with photoprotective green fluorescent protein expression as potential drivers of

balancing selection for color polymorphism in reef corals, *Frontiers in Marine Science*, 5: 11.

Raskoff, K. (2013) The design and construction of a low cost recirculating seawater system for student or research use. Western Society of Naturalists Conference, November 2013, Oxnard CA.

Rodgers, G.G., Tenzing, P. and Clark, T.D. (2016) Experimental Methods in Aquatic Respirometry: The Importance of Mixing Devices and Accounting for Background Respiration, *Journal of Fish Biology*, 88: 65-80.

Roth, M. S., Padilla-Gamiño, J. L., Pochon, X., Bidigare, R. R., Gates, R. D., Smith, C. M. and Spalding, H. L. (2015) Fluorescent proteins in dominant mesophotic reef-building corals, *Marine Ecology Progress Series*, 521: 63-79.

Sachs, J.L. and Wilcox, T.P. (2006) A shift to parasitism in the jellyfish symbiont *Symbiodinium microadriaticum*, *Proceedings of the Royal Society B*, 273: 425-429.

Salih, A., Larkum, A., Cox, G., Kühl, M. and Hoegh-Guldberg, O. (2000) Fluorescent pigments in corals are photoprotective, *Nature*, 408: 850-853.

Saunders, B.K. and Muller-Parker, G. (1997) The effects of temperature and light on two algal populations in the temperate sea anemone *Anthopleura elegantissima* (Brandt, 1835), *Journal of Experimental Biology and Ecology*, 211: 213-224.

Sánchez-Zurano, A., Gómez-Serrano, C., Acién-Fernández, F. G., Fernández-Sevilla, J. M. and Molina-Grima, E. (2020) A novel photo-respirometry method to characterize consortia in microalgae-related wastewater treatment processes, *Algal Research*, 47: 101858.

Sebens, K. P., Helmuth, B., Carrington, E. and Agius, B. (2003) Effects of water flow on growth and energetics of the scleractinian coral *Agaricia tenuifolia* in Belize, *Coral Reefs*, 22: 35-47.

Sherpa, A.S., Schossow, D., Lenning, M., Marsh, P., Garzon, N., Hofsteen, P., Cao, H., Yang, J., Xu, X., Nguyen, T.T.V., Tran, N.C., Bui, T.T. and Chu, D.T. (2017) Novel Apparatus of Simultaneous Monitoring of Electrocardiogram in Awake Zebrafish, *Proceedings of IEE Sensors*, 2017-December: 1-3.

Smith, E. G., D'Angelo, C., Sharon, Y., Tchernov, D. and Wiedenmann, J. (2017) Acclimation of symbiotic corals to mesophotic light environments through wavelength transformation by fluorescent protein pigments, *Proceedings of the Royal Society B*, 284: 20170320. <https://doi.org/10.1098/rspb.2017.0320>.

Smith, E. G., D'Angelo, C.D., Salih, A. and Wiedenmann, J. (2013) Screening by coral green fluorescent protein (GFP)-like chromoproteins supports a role in photoprotection of zooxanthellae, *Coral Reefs*, 32: 463-474.

Steele, R.D. (1976) Light intensity as a factor in the regulation of the density of symbiotic zooxanthellae in *Aiptasia tagetes* (Coelenterata, Anthozoa), *Journal of Zoology*, 179(3): 387-405.

Steffensen, J.F. (1989) Some Errors in Respirometry of Aquatic Breathers: How to Avoid and Correct for Them, *Fish Physiology and Biochemistry*, 6(1): 49-59.

Svendsen, M. B. S., Bushnell, P. G. and Steffensen, J. F. (2016) Design and setup of intermittent-flow respirometry system for aquatic organisms, *Journal of Fish Biology*, 88: 26-50.

Tait, L. W. and Schiel, D. R. (2010) Primary productivity of intertidal macroalgal assemblages: comparison of laboratory and *in situ* photorespirometry, *Marine Ecology Progress Series*, 416: 115-125.

Taylor, D.L. (1969) On the regulation and maintenance of algal numbers in zooxanthellae-coelenterate symbiosis, with a note on the nutritional relationship in *Anemonia sulcata*, *Journal of the Marine Biological Association of the United Kingdom*, 49(4): 1057-1065.

Taylor, J. A. and Lloyd, J. (1992) Sources and Sinks of Atmospheric CO₂, *Journal of Botany*, 40(5): 407 – 418.

Thomas, M., Martin, B., Kowarski, K., Gaudet, B. & Matwin, S. Marine mammal species classification using convolutional neural networks and a novel acoustic representation. *European Conference on Machine Learning and Principles and Practice of Knowledge Discovery in Databases*, Würzburg, Germany (2019).

Trenberth, K. E. (2018) Climate change caused by human activities is happening and it already has major consequences, *Journal of Energy & Natural Resources Law*, 36(4): 463-481.

- Tsutsui, K., Shimada, E., Ogawa, T. and Tsuruwaka, Y. (2016) A novel fluorescent protein from the deep-sea anemone *Cribrinopsis japonica* (Anthozoa: Actiniaria), *Scientific Reports*, 6: 23493.
- Verde, E.A. and McCloskey, L.R. (2007) A Comparative Analysis of the Photobiology of Zooxanthellae and Zoochlorellae Symbiotic with the Temperate Clonal Anemone *Anthopleura elegantissima* (Brandt). III. Seasonal Effects of Natural Light and Temperature on Photosynthesis and Respiration, *Marine Biology*, 152: 775-792.
- Weidenmann, J., Leutenegger, A., Gundel, S., Schmitt, F., D'Angelo, C. and Funke, W. (2007) Long-term monitoring of space competition among fluorescent and nonfluorescent sea anemones in the Mediterranean Sea, *Journal of the Marine Biological Association of the United Kingdom*, 87(4): 851-852.
- Weinbauer, G., Nussbaumer, V. and Patzner, R. A. (1981) Studies on the relationship between *Inachus phalangium* Fabricus (*Maiidae*) and *Anemonia sulcata* Pennant in their natural environment, *Marine Ecology*, 3(2): 143-150.
- Wooldridge, S.A. (2010) Is the coral-algae symbiosis really 'mutually beneficial' for the partners?, *Bioessays*, 32(7): 615-625.
- Xiang, T., Lehnert, E., Jinkerson, R.E., Clowez, S., Kim, R.G., DeNofrio, J.C., Pringle, J.R. and Grossman, A.R. (2020) Symbiont population control by host-symbiont metabolic interaction in Symbiodiniaceae-cnidarian associations, *Nature Communications*, 11:108.
- Yamashiro, H. and Nishihara, M. (1995) Phototaxis in Fungiidae corals (Scleractinia), *Marine Biology*, 124: 461-465.